





Learning from Hypervectors: A Survey on Hypervector Encoding

Sercan Aygun , *Member, IEEE*, Mehran Shoushtari Moghadam , *Student Member, IEEE*,

M. Hassan Najafi , *Member, IEEE*, and Mohsen Imani , *Member, IEEE*

Abstract—Hyperdimensional computing (HDC) is an emerging computing paradigm that imitates the brain’s structure to offer a powerful and efficient processing and learning model. In HDC, the data are encoded with long vectors, called hypervectors, typically with a length of 1K to 10K. The literature provides several encoding techniques to generate orthogonal or correlated hypervectors, depending on the intended application. The existing surveys in the literature often focus on the overall aspects of HDC systems, including system inputs, primary computations, and final outputs. However, this study takes a more specific approach. It zeroes in on the HDC system input and the generation of hypervectors, directly influencing the hypervector encoding process. This survey brings together various methods for hypervector generation from different studies and explores the limitations, challenges, and potential benefits they entail. Through a comprehensive exploration of this survey, readers will acquire a profound understanding of various encoding types in HDC and gain insights into the intricate process of hypervector generation for diverse applications.

Index Terms—Hyperdimensional computing, hypervector generation, hypervector mapping, signal encoding.

I. INTRODUCTION

HYPERDIMENSIONAL computing (HDC) is a burgeoning computing paradigm that has recently surged in popularity. HDC emulates brain-like processing and finds application in various cognitive tasks [1] from text analysis [2], to recommendation systems [3], genome research [4], security issues [5] and Internet of Things (IoT) applications [6], to name a few. HDC is a compelling computing paradigm that has gained popularity for its unconventional approach to data processing alongside other emerging computing paradigms such as stochastic computing (SC), unary computing, approximate computing, and quantum computing [7], [8]. In HDC, the (scalar) data are represented by encoding binary (or bipolar) values into long *hypervectors* (\mathcal{HVs}). In other words, the encoding process maps the input data from the scalar domain to a hyperspace. The \mathcal{HVs} enable straightforward processing through simple logic elements, thereby obviating the need for complex circuit elements. Basic arithmetic operations, such as multiplication and addition for binary \mathcal{HVs} , are achieved using logical XOR and counters. One significant advantage of processing data with long \mathcal{HVs} is the robustness they offer against soft errors [9], thus addressing error-prone concepts such as bit significance (most- and least-significant bits) and the sign bit in conventional binary radix representation. The fault-robust property of HDC has particularly demonstrated its advantage in emerging memory environments, including in-memory computing (IMC), resistive RAM-based processing, and FinFET-based architectures [10], [11]. The ability to endure in such advanced computing setups underscores the HDC’s potential as a dependable computing solution.

This work was supported in part by the National Science Foundation (NSF) under Grant 2127780 and Grant 2019511; in part by the Semiconductor Research Corporation (SRC) Task under Grant 2988.001; in part by the Department of the Navy, Office of Naval Research, under Grant N00014-21-1-2225 and Grant N00014-22-1-2067; in part by the Air Force Office of Scientific Research; in part by the Louisiana Board of Regents Support Fund under Grant LEQSF(2020-23)-RD-A-26; and in part by Cisco, Xilinx, and NVIDIA.

Sercan Aygun is with Sch. Comp. and Info., Univ. of Louisiana at Lafayette, 70503 Lafayette, LA, USA (e-mail: sercan.aygun@louisiana.edu).

Mehran Shoushtari Moghadam is with Sch. Comp. and Info., Univ. of Louisiana at Lafayette, 70503 Lafayette, LA, USA (e-mail: mehran.shoushtari-moghadam1@louisiana.edu).

M. Hassan Najafi is with Sch. Comp. and Info., Univ. of Louisiana at Lafayette, 70503 Lafayette, LA, USA (e-mail: najafi@louisiana.edu).

Mohsen Imani is with Comp. Sci. and Eng., Univ. of California Irvine, 92697 Irvine, CA, USA, (e-mail: m.imani@uci.edu).

TABLE I
PREVIOUS SURVEY STUDIES ON HDC

Year	Authors	Title
2023	Ma et al. [5]	Robust Hyperdimensional Computing Against Cyber Attacks and Hardware Errors: A Survey
2023	Chang et al. [12]	Recent Progress and Development of Hyperdimensional Computing (HDC) for Edge Intelligence
2022	Kleyko et al. [13]	A Survey on Hyperdimensional Computing aka Vector Symbolic Architectures, Part II: Applications, Cognitive Models, and Challenges
2022	Kleyko et al. [14]	A Survey on Hyperdimensional Computing aka Vector Symbolic Architectures, Part I: Models and Data Transformations
2022	Hassan et al. [15]	Hyper-Dimensional Computing Challenges and Opportunities for AI Applications
2020	Lulu and Parhi [16]	Classification Using Hyperdimensional Computing: A Review
2017	Gritsenko et al. [17]	Neural Distributed Autoassociative Memories: A Survey

The fundamental data units within HDC systems consist of vectors comprising values of +1 (representing logic-1) and −1 (representing logic-0). To encode data, \mathcal{HVs} of up to 10,000 bits in length have been employed. Some recent endeavors focused on reducing the size of the \mathcal{HVs} (D) to enhance application accuracy. Longer \mathcal{HVs} yield more effectively embedded information. Alongside determining the size (D), the encoding type is another pivotal factor directly impacting accuracy. Typically, data are encoded into random \mathcal{HVs} that are *orthogonal* to each other. The concept of orthogonality is crucial in HDC as it allows representing unique features/symbols such as a letter in a text processing system, a pixel position in an image in a cognitive task [18], or a time series in a voice recognition task [19]. The phenomenon of orthogonality (or non-orthogonality in certain cases) significantly influences \mathcal{HV} generation and, in turn, the accuracy of the system. Notably, randomly generated vectors exhibit a degree of *near* orthogonality to each other [20]. Therefore, these randomly generated and pre-allocated vectors effectively represent symbols in HDC systems, serving as atomic data primitives within the application.

Various methods have been employed in the literature to achieve nearly-orthogonal \mathcal{HVs} . Among these, one prominent technique involves initiating the process with an initial seed vector and subsequently determining additional vectors through random bit-flip operations [21]. This methodology yields correlated vectors for related scalars, while distant scalars result in uncorrelated vectors. It is noteworthy that the specific method of vector generation varies depending on the nature of the data under consideration and the specific application context. For instance, in the context of a language classification problem [2], vectors are generated using a random approach to ensure that the symbols (specifically, letters) constituting the language class are (near) orthogonal to each other. Furthermore, to maintain orthogonality within each subset of sentences referred to as *N-grams*, logical shifts are applied to the letter \mathcal{HVs} [2]. This procedure effectively preserves the contextual relationships within the language, thereby facilitating the language classification task.

Our survey study fills a notable gap in the existing literature, namely the absence of a survey specifically focused on the \mathcal{HV} generation and encoding aspect of HDC systems. While previous surveys and benchmark studies have effectively presented the overall structure, applications, and motivations of HDC (see Table I), this work delves into the intricate process of \mathcal{HV} generation. A recent survey by Chang et al. [12]

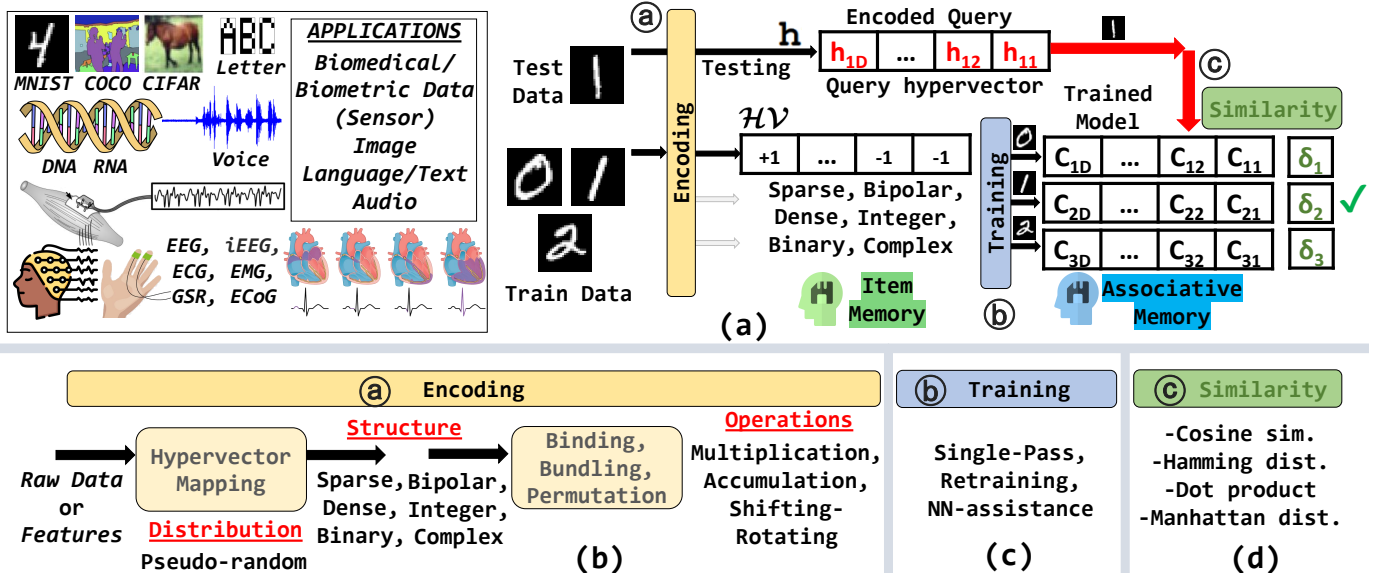


Fig. 1. A general overview of an HDC system targeting classification. (a) From applications to learning and classifying steps: (a) Encoding the incoming data. (b) Training using the whole bunch of input dataset, (c) Similarity check between class-based $\mathcal{H}\mathcal{V}$ s (C_{class}) and query hypervector. Mainly, HDC systems target biomedical/biometrics applications, image and text processing, and some sensor data processing, also considering continuous signals like audio (VoiceHD [19]). Famous datasets used in HDC prior works generally include (i) *UCI-HAR* (Human Activity Recognition Using Smartphones [22]) like [23], [24], *THRIFTY* [25], *MuTa-HDC* [26], [27], [28], [29], (ii) *ISOLET* (Spoken Letters [30]) like [31], *HDnn-PIM* [32], *tiny-HD* [6], (iii) *PMAMP* (Physical Activity Monitoring, [33]) like *OpenHD* [34], *QuantHD* [35], *HD Torch* [36], (iv) *FACE* (Caltech256 dataset [37]) like *AdaptHD* [38], [25], [34], (v) *MNIST* (Modified National Institute of Standards and Technology database [39]) like [40], [41], [35], [42], [40], [43], [44], [45], (vi) *CARDIO* (Cardiotocography [46]) like [25], *Store-n-Learn* [47], [48], (vii) *CIFAR* (Canadian Institute For Advanced Research [49]) [42], [50], [51], [32], [52]. Biomedical data processing applications lead the trend, and EEG (electroencephalogram) [53]–[55], ECG (electrocardiogram) [56], iEEG (intracranially recorded EEG signals) [57], EMG (Electromyography) [58], GSR (Galvanic Skin Response) [59], and ECoG (electrocardiography) [54] are well-known examples of HDC applications. The distribution of the $\mathcal{H}\mathcal{V}$ s is pseudo-random for orthogonality; if the correlation is needed for closer numerical values of input data, $\mathcal{H}\mathcal{V}$ mapping of two close values yields relatively similar distributions. The operations here for binding are given as a general operation. Literature has different binding examples: *blockwise-circular convolution* [60], *circular convolution* [61], *geometric product* [62] and *component-wise modular addition* [29], [63]. (b) The details of vector mapping; raw data or extracted features can be used. The obtained $\mathcal{H}\mathcal{V}$ s are performed for the remaining encoding operations, such as binding, bundling, and permutation. (c) The training procedure can have a 1-data-1-pass conception or 1-data-multiple-pass to retrain the model. Several works have neural network assistance [41], [64]. (d) Similarity measurement is based on the well-known binary comparison metrics.

reviewed HDC from the vantage point of edge intelligence and cloud collaboration, encompassing discussions on security-privacy issues. Within the realm of HDC research, Chang et al. [12] categorize the hardware environment into three primary domains of microprocessor, FPGA, and computing-in-memory (CIM). Although the listed studies on hardware comparisons of HDC implementations contain some information on the encoding process, an explicit emphasis on the crucial aspect of $\mathcal{H}\mathcal{V}$ generation is necessary. Another recent two-part survey by Kleyko et al. [13], [14] offers a highly comprehensive analysis. The first part of their survey [14] focuses on exploring the opportunities for data transformation during $\mathcal{H}\mathcal{V}$ encoding. The primary aim of this part is to equip the readers with a foundational knowledge of basic notations, computational models, and input transformations. They further provide an overview of the HDC models with a specific emphasis on essential HDC operations, such as binding, unbinding, and superposition. Lulu and Parhi [16], in their state-of-the-art (SOTA) survey, define two main benchmark metrics for HDC: I) *accuracy*, and II) *efficiency*. The *accuracy* depends on three factors: *encoding*, *retraining*, and *non-binary*. They discuss *encoding* as one of the critical factors affecting accuracy. *Efficiency*, on the other hand, is discussed under two categories: algorithm and hardware. Three factors affect the algorithm: binarization, quantization, and sparsity. Therefore, the first step for encoding, *$\mathcal{H}\mathcal{V}$ generation*, affects accuracy and efficiency depending on the vector distribution (sparse or dense). In addition to these surveys and benchmarks, Kleyko et al. [14] highlight the studies in [65], [66], and [67] as tutorial-like introductory articles on HDC.

Our study is centered on a concise and comprehensive survey with the primary objective of elucidating the *encoding* process in HDC systems. Additionally, it discusses the potent capabilities of conducting computations across the vector-based paradigms such as HDC and SC at the $\mathcal{H}\mathcal{V}$ generation level. The structure of this study is as follows: Section II provides a comprehensive overview of HDC systems and the relevant background information. Section III delves into the

intricacies of binary coding, elucidating the functionalities of the *Encoding Module* in HDC. Section IV consolidates HDC’s technical and hardware aspects, drawing upon application-centric prior investigations and highlighting crucial encoding features. Section V discusses the challenges, limitations, and potentials of the encoding procedure in HDC systems, incorporating insights from diverse research endeavors. Section VI further offers practical guidance to the reader with a list of available platforms and a summary of SOTA works. Finally, Section VII discusses the study’s conclusions and findings.

II. AN OVERVIEW OF HDC SYSTEMS

In this section, we provide the fundamental background for understanding HDC systems. Firstly, we present an overview of the key sub-modules that constitute HDC. Fig. 1 shows a general depiction of the HDC system, consisting of three primary steps. The first step, denoted in Fig. 1 (a), is the *Encoding* process. After mapping the input data (or features) to the atomic $\mathcal{H}\mathcal{V}$ s, the encoding stage performs some arithmetic operations on the $\mathcal{H}\mathcal{V}$ s. These operations are categorized into *Binding* (*Multiplication*), *Bundling* (*Accumulation*) and *Permutation* (*Shift-Rotate*). The second step, shown in Fig. 1 (b), corresponds to the *Training* phase. In this step, all of the related $\mathcal{H}\mathcal{V}$ s from the same category are merged together to create a unique class $\mathcal{H}\mathcal{V}$ to represent any unique data class. Lastly, the third step, depicted as in Fig. 1 (c), involves *Similarity* calculation. This phase deals with measuring the similarity (e.g. cosine, hamming-distance, dot product, etc.) between the newly encoded hypervector as the test input to the model with the class $\mathcal{H}\mathcal{V}$ s. Thus, at its core, the HDC framework establishes a general outline for creating a learning model and classifying incoming data into their respective classes.

This survey study focuses on the encoding step in Fig. 1 (b) with detailed insights targeting the initial vector mapping. Essentially, the initial stage of encoding entails the embedding of available data into vectors, also known as “mapping.” This process, referred to as *$\mathcal{H}\mathcal{V}$ generation* or *projection*, generates

TABLE II
FIRST GLANCE OF PRIOR HDC ARTS CLASSIFIED BASED ON PROMINENT APPLICATIONS.

Key Topic	SOTA Works
Biomedical/Biometrics	[68], [64], [54], [20], [69], [56], [68], [35], [70], [71], [72], [73], [58], [74], [75], [59], [76], [77], [78], [79], [80], [81], [82], [83], [84], [47], [85], [48], [55], [57], [53], [86]
Image Process./Computer Vision	[87], [1], [35], [70], [71], [51], [73], [88], [89], [41], [42], [90], [91], [92], [93], [94], [95], [96], [97], [83], [98], [44], [45], [32], [52], [99], [100]
Memory-centric Computing	[101], [1], [102], [72], [103], [104], [11], [105], [32], [106], [107], [108], [109], [110], [111], [112], [113], [114], [115], [47], [116]
Security/Reliability Issues	[117], [88], [5], [5], [114], [118], [119], [120], [121], [122], [123], [124], [125], [126]
Inter-computing Collab.*	[102], [116], [127], [128], [50], [129], [130], [131], [132]
Language/Text Processing	[10], [2], [133], [89], [134], [119], [93], [94], [95]
DNA Processing	[135], [4], [136], [137], [138], [139]

*: Inter-computing collaborations deal with exploiting Quantum Computing, Neuromorphic Computing, Unary Computing, and **Stochastic Computing** under the umbrella of the Emerging Computing paradigm in the context of Hyperdimensional Computing. In Section IV, we further explain the importance of **Stochastic Computing** on the HDC performance utilizing LD-sequences to generate high-quality $\mathcal{H}\mathcal{V}$ s.

a vector based on a (pseudo-)random source, resulting in a comprehensive representation of the data. While the literature often labels this step as *random $\mathcal{H}\mathcal{V}$ generation*, our emphasis in Section IV lies on obtaining orthogonal vectors, considering vector design qualities beyond mere pseudo-randomness by exploring other high-quality distributions, such as low-discrepancy (LD) distribution [140] with quasi-random sequences [141], [142] among others. The structure of the resulting vector can change with the computation model; it may take on binary forms (logic-1, logic-0) or bipolar representations (+1, -1). Moreover, various structural variations in the vectors are possible, including *sparse* and *dense* representations [14], as illustrated in Fig. 1 (b).

HDC offers remarkable efficiency, emerging as a promising alternative to traditional machine learning (ML) models. HDC achieves this through four key aspects: ① streamlined arithmetic operations [102], ② non-iterative learning [143], ③ model tuning without optimization [47], and ④ compact model size [129]. In contrast, conventional neural networks (NNs) rely on three fundamental operations during the learning phase: (i) multiplication, (ii) addition, and (iii) activation. Conversely, HDC's model acquisition involves the simple logical operations of (i) multiplication or binding using XORs; (ii) addition or bundling utilizing population counters, and (iii) binarization employing comparators ①. Binding and bundling are part of the encoding phase, and permutation operations via shifting may be needed to maintain consistent $\mathcal{H}\mathcal{V}$ orthogonality between operations. The final model in HDC is attained solely through these foundational steps, while conventional ML with NNs requires optimization through operation-intensive partial derivations and model updates ②, ③). As indicated in Fig. 1 (c), HDC uses single-pass learning optionally with a simple retraining methodology [42]. Training data is evaluated once in most approaches, and the holistic model is obtained. Some HDC examples may include NN assistance to boost learning efficiency [64]. The HDC model consists of a set of $\mathcal{H}\mathcal{V}$ s, each representing a class vector for the classification task. Unlike using positional weights in matrices connecting numerous neurons across consecutive layers in NN systems, HDC uses D -sized $\mathcal{H}\mathcal{V}$ s for each class ④). When the training is complete, the obtained model is checked with the testing data as in conventional ML systems. The encoding in HDC is a global step that is also applied to the testing data. For any class, the query data is encoded into a D -sized hypervector. In the decision phase, the query vector is compared with each $\mathcal{H}\mathcal{V}$ of a class already trained in the model. Fig. 1 (d) shows different similarity measures used for checking the similarity between query hypervector and the class $\mathcal{H}\mathcal{V}$ s.

The simplicity and efficiency of the HDC paradigm, along with its single-pass training advantage have spurred its adoption in various applications. Table II presents an overview of prior HDC studies across diverse domains. Biomedical/Biometric, Image Processing, In-Memory Computation, Security, and Language Processing have been the primary focus of HDC research. However, there remains a relatively limited number of works exploring HDC applications in the DNA domain, which presents an open research topic with significant potential for further investigation.

III. HYPERVECTOR ($\mathcal{H}\mathcal{V}$) MAPPING

The core focus of most prior HDC studies centers on the overall encoding procedure, which typically emphasizes vector arithmetic. However, from the perspective of learning within the realm of data science, the initialization of vectors holds a crucial aspect in shaping the overall model. In their SOTA survey on HDC, Kleyko et al. acknowledge the existing research [65], [67], [144]–[147] and underscore the lack of a survey work dedicated to $\mathcal{H}\mathcal{V}$ for various types of data representations, such as numeric, 2D image, sequence, and others [14]. Consequently, the investigation of vector generation techniques tailored to specific data types has remained relatively overshadowed by other aspects of HDC. Undoubtedly, the encoding process using $\mathcal{H}\mathcal{V}$ s constitutes a critical step that profoundly impacts both the accuracy and efficiency of HDC. The dynamic generation of $\mathcal{H}\mathcal{V}$ s using an efficient hardware architecture is critical both for overall hardware cost and on-edge learning [92]. The overall effectiveness and learning performance of the HDC models heavily relies on the quality of encoding the input data into $\mathcal{H}\mathcal{V}$ s [76]. Achieving accurate and efficient encoding is vital to ensuring the reliable and high-performance operation of HDC in various applications [12]. Kleyko et al. delve into the structure of the $\mathcal{H}\mathcal{V}$ s, such as dense, sparse, and binary. They discuss the trade-offs involved in the selection of $\mathcal{H}\mathcal{V}$ density and some mapping characteristics [89]. Such insights shed light on optimizing the encoding process and its impact on HDC performance and applications.

Two well-known encoding methods commonly found in the literature are the *record-based* and *N -gram based* approaches [58], [68], [148], [149]. For each input feature i , the former employs position $\mathcal{H}\mathcal{V}$ s denoted as \mathcal{P}_i , which exhibit orthogonality with respect to each other, and level $\mathcal{H}\mathcal{V}$ s denoted as \mathcal{L}_i , which demonstrate correlation for neighboring pairs. The individual $\mathcal{H}\mathcal{V}$ of a specific class is generated by the summation of the element-wise multiplication (\oplus : logical XOR) between the *position* and *level* $\mathcal{H}\mathcal{V}$ s for each feature (or raw data element). The resulting single $\mathcal{H}\mathcal{V}$ for the total number of features (N) is represented as \mathcal{H} , and is calculated as follows:

$$\mathcal{H} = \sum_{i=1}^N (\mathcal{L}_i \oplus \mathcal{P}_i) \quad (1)$$

The *N -gram based* method leverages the permutation operation (π) for each level $\mathcal{H}\mathcal{V}$ (\mathcal{L}_i). In this approach, the resulting class $\mathcal{H}\mathcal{V}$ is generated by element-wise multiplication (XORing) of the permuted level $\mathcal{H}\mathcal{V}$ s. The final $\mathcal{H}\mathcal{V}$ in this case is represented as follows:

$$\mathcal{H} = \mathcal{L}_1 \oplus \pi \mathcal{L}_2 \oplus \dots \oplus \pi^{N-1} \mathcal{L}_N \quad (2)$$

In a similar manner, Salamat et al. [150] proposed a novel $\mathcal{H}\mathcal{V}$ generation method for every feature vector A_i containing N elements of the form $A_i = \{a_1, a_2, \dots, a_N\}$, where each a_i demonstrates a feature value \mathfrak{F}_i with l levels as $a_i \in (\mathfrak{F}_1, \mathfrak{F}_2, \dots, \mathfrak{F}_l)$. In this case, the lowest feature value (\mathfrak{F}_1) is assigned a random $\mathcal{H}\mathcal{V}$ called \mathcal{H}_1 with size D and the highest feature value (\mathfrak{F}_l) is assigned a random $\mathcal{H}\mathcal{V}$ called \mathcal{H}_l by randomly flipping $D/2$ bits. Starting from the first $\mathcal{H}\mathcal{V}$ (corresponding to the lowest feature value), the remaining $\mathcal{H}\mathcal{V}$ s are generated by flipping $\frac{D/2}{l-1}$ bits at

each step. Afterward, each feature value \mathfrak{F}_i is mapped to its associated \mathcal{HV} as \mathcal{H}_i . In order to take the position and/or temporal position of each input feature into account, the permutation operation (π) is performed. The final \mathcal{HV} denoted as \mathcal{H}_C is generated by aggregating (bundling) the permuted \mathcal{HVs} as:

$$\mathcal{H}_C = \sum_{t=1}^D \pi^{(t)} \mathcal{H}_t \quad (3)$$

The authors in [150] further proposed to perform permutation operation on each segment of \mathcal{S} size instead of per bit permutation. The advantage of this method is the utilization of fewer Blocked RAMs (BRAMs) in FPGA. Accordingly, the work in [68] proposed a novel multi-encoder method to take advantage of *record-based* and *N-gram-based* encoding methods, which adaptively selects the proper encoding method according to the complexity of the input data and reducing the dimension of the \mathcal{HVs} to increase the hardware efficiency in terms of power consumption and execution time.

In vector mapping from scalars, Rachkovskij et al. [151] thoroughly discuss the opportunities of sparse binary distributed encoding. They discuss thermometric encoding, partially distributed floret encoding, partially distributed multi-floret encoding, distributed stochastic encoding, subtractive-additive encoding, and encoding by concatenation.

For \mathcal{HV} manipulation, Schmuck et al. [152] discuss a generic module that replaces costly memory storage with cheaper logical operations to rematerialize seed \mathcal{HVs} , facilitating the construction of composite \mathcal{HVs} without the need for additional memory. They introduce an innovative approach for the majority gate application, utilizing a \mathcal{HV} manipulator module to perform approximate majority gating incrementally, enabling continuous operation in the binary space for efficient on-chip learning. They perform a design space exploration to showcase various functionally equivalent HDC architectures, achieving substantial area and throughput improvements compared to a baseline architecture. They implement the Pareto optimal HDC architecture on Xilinx UltraScale FPGAs, utilizing only 18340 configurable logic blocks (CLBs). This optimized architecture achieves impressive improvements, with a 2.39 \times reduction in area and a remarkable 986 \times increase in throughput when compared to a baseline HDC architecture.

Symbolic representations, such as the letter processing example, require orthogonal, i.e., dissimilar vectors. However, if the application involves numerical data, then similarity or correlation between some data points is required. For dissimilarity, random dense vectors with 50% of the binary values with 1s are utilized for orthogonality. If the “1” and “0” vector elements are roughly equiprobable, then the vector is called a *dense vector*. For numerical data, closer values might need similar \mathcal{HV} representations, and a sparse vector is a better choice. If each \mathcal{HV} differs from the other by a few bits, then the sparsity can be obtained in the vector representation [153]–[155].

Hersche et al. [156], and Cannings and Samworth [84] proposed random projection methods using dense bipolar vectors (with +1s and -1s) for encoding \mathcal{HVs} . This encoding type may be inefficient for hardware implementations because of massive addition/multiplication operations. Instead of using random projection [157] with dense \mathcal{HVs} , utilizing sparse random projection would lead to improving the efficiency by using $s\%$ (known as sparsity factor) of the \mathcal{HV} elements to be generated randomly. Choosing the proper sparsity factor can significantly reduce the number of arithmetic operations. Further improvement could be achieved by preserving the benefit of sparsity in random projection and omitting random access in generating \mathcal{HVs} as a hardware-friendly approach with predefined non-zero indices of \mathcal{HVs} [71], [87]. Random indexing was proposed as a method of projecting data elements onto \mathcal{HV} space for the text contexts [2], [158]. In this method, each \mathcal{HV} is generated by a small fraction of randomly distributed +1s and -1s and remaining elements of zeros (as a sparse \mathcal{HV}) for each element of data.

Basaklar et al. [76] proposed an optimized \mathcal{HV} design with lower dimensionality compared to conventional high

dimension HDC for resource-restrained wearable IoT devices. They assumed a baseline HDC structure with input features $F = \{f_1, f_2, \dots, f_N\}$ and S training samples. Each training sample x_s in sample space S is an N -tuple of the form $x_s = \{x_s^1, x_s^2, \dots, x_s^N\}$ in which each x_s^n is the corresponding value of the feature f_n . To construct the sample \mathcal{HVs} , first, the level \mathcal{HVs} are generated by quantizing each feature value to M levels. The first level of the f_n is assigned to a random bipolar D -dimension \mathcal{HV} (L_n^1) and the other consecutive level \mathcal{HVs} ($L_n^m, \forall m \in \{1, \dots, M\}$) are generated by randomly flipping $b = D/2(M-1)$ bits. Finally, the sample \mathcal{HV} (X_s) is generated by adding the associated level \mathcal{HV} assigned to the related input feature as:

$$X_s = \sum_{n=1}^N L_n^m \forall m \in \{1, \dots, M\} \quad (4)$$

In a similar manner, the class \mathcal{HVs} are generated by combining sample \mathcal{HVs} belonging to the same class. The proposed method employs varying numbers of bit flips for each consecutive level of \mathcal{HVs} , treating the generation of \mathcal{HVs} as a multi-objective optimization problem. The objectives are twofold: 1) maximizing the training accuracy, and 2) minimizing the similarity between different classes. To achieve significant dimensionality reduction in \mathcal{HVs} , the approach utilizes the 2D t -distributed Stochastic Neighbor Embedding (*t-SNE*) algorithm, which is highly efficient in terms of hardware area and power consumption, for nonlinearity reduction. In contrast to previous works that used *record-based* encoding and *N-gram-based* encoding methods for \mathcal{HVs} [149], their method generates sample \mathcal{HVs} by simply adding the level \mathcal{HVs} together.

Several non-linear encoding methods [159], [160] have been proposed in the literature inspired from the Radial Basis Function (RBF) kernel trick. These methods, introduced in various works such as Dual [105], FebHD [161], DistHD [162], NeuralHD [163], RE-HFDC [28], and ManiHD [164], encode each dimension of the data by calculating the dot product of the feature vector (F) with a randomly generated vector (B_i) sampled from a Gaussian distribution with mean $\mu = 0$ and standard deviation $\sigma = 1$, denoted as $h_i = \cos(B_i \cdot F)$. The final encoded \mathcal{HV} is binarized using a sign function. The same method has been employed in DistHD and CyberHD [122] to identify and regenerate the insignificant dimensions, resulting in reduced dimensionality in the \mathcal{HVs} and enhancing the overall system efficiency. In DistHD, the \mathcal{HVs} are generated based on the form $h_i = \cos(B_i \cdot F + c) \times \sin(B_i \cdot F)$ with $c \sim \text{Uniform}[0, 2\pi]$.

The method proposed by Kleyko et al. [165] involves using a base random \mathcal{HV} and performing multiple circular shifts in each iteration to generate orthogonal \mathcal{HVs} . In [89], two types of encoding are employed for black-and-white images of letters and hand gesture recognition from a sequence of electromyography (EMG) signals. In the first encoding method (*Dissimilar Distributed Encoding*), each feature is randomly assigned to a binary dense \mathcal{HV} . Based on the feature value being 0 or 1, the corresponding \mathcal{HV} undergoes a circular 0-bit or 1-bit shift, respectively. All of these \mathcal{HVs} will be orthogonal to each other, ensuring distinctiveness. In the second encoding method (*Distance-Preserving Distributed Encoding*), each feature is assigned to a \mathcal{HV} with a random number of bit-flips. Unlike the first method, the adjacent \mathcal{HVs} exhibit similarities to each other as their distance is preserved.

The SOTA research follows two general procedures for encoding 2D images: 1) utilizing raw pixel values [166], and 2) leveraging ML techniques to extract and utilize features [35], [69], [131]. The former approach results in lightweight hardware design outputs but may suffer from lower accuracy. On the other hand, the latter approach achieves higher accuracy but requires feature engineering and requires hardware considerations for the feature extraction process. In the context of pixel-based processing, the SOTA works explore two types of information [16]: (i) pixel values, often referring to grayscale values, and (ii) pixel positions. The first one involves generating level \mathcal{HVs} with numerical significance, while the

second requires orthogonal $\mathcal{H}\mathcal{V}$ s to represent unique pixel positions.

An intriguing method, fractional power encoding, is discussed in [14] for encoding 2D images. This approach involves producing two randomly assigned base $\mathcal{H}\mathcal{V}$ s, denoted as \mathcal{A} and \mathcal{B} , for the x and y axes, respectively. Subsequently, for each position (u, v) in the image, the corresponding $\mathcal{H}\mathcal{V}$ denoted as \mathcal{W} is computed by raising the base $\mathcal{H}\mathcal{V}$ to the power of the respective coordinate values (bound together). Thus, the expression for the resulting $\mathcal{H}\mathcal{V}$ at position (u, v) is as follows:

$$\mathcal{W} = \mathcal{A}^u \oplus \mathcal{B}^v \quad (5)$$

Table III presents a comprehensive overview of prior works, showcasing various $\mathcal{H}\mathcal{V}$ mapping and encoding styles and the sources used for $\mathcal{H}\mathcal{V}$ generation. The majority of the prior approaches adopt random source functions, such as the `rand` function in MATLAB or Python, to generate $\mathcal{H}\mathcal{V}$ s. However, certain prior works, specifically [129] and [50], explore the use of LD-sequences as the source for $\mathcal{H}\mathcal{V}$ generation. These works demonstrate significantly higher accuracy for HDC language processing [129] and HDC image classification [50]. The higher accuracy is attributed to the inherent determinism and enhanced orthogonality by employing LD-sequences compared to random-based $\mathcal{H}\mathcal{V}$ generation methods.

IV. NEW PERSPECTIVES ON HYPERVECTOR MAPPING

This section explores some novel opportunities for HDC encoding. Specifically, it addresses the pseudo-random nature of pre-allocated or dynamically generated $\mathcal{H}\mathcal{V}$ s, which requires identifying the best-performing hypervectors through multiple iterations. To investigate this, we employ a language classification problem [129] as a reference and make a pertinent observation concerning the random procedure. In the context of the language classification problem, the SOTA accuracy [2] achieved on the Europarl Parallel Corpus dataset [202] is reported as 97.1%. This performance is attained using $D=10,000$ and $N=4$ -gram parameters, with the $\mathcal{H}\mathcal{V}$ s being randomly assigned. However, an intriguing discovery is made when employing *quasi-random* numbers, such as Sobol Sequences [140], [203], [204] for vector generation. These sequences previously showed significant accuracy improvements for SC systems [142]. By utilizing only one iteration of vector generation without resorting to any best candidate iterative selection, the accuracy increases by 0.2%. However, upon decreasing D to 256, a significant disparity in average accuracy emerges between the pseudo-random approach, yielding 69.24%, and the LD-based quasi-random vector generation, achieving an impressive 79.03% classification rate. This compelling result underscores the potential of LD-based quasi-random vector generation as a promising technique for enhancing vector mapping in HDC encoding. Building on these findings, there arises an exciting opportunity to leverage SC [205] and its deterministic processing avenue [142], [206]. By incorporating SC principles into the HDC vector generation process, we can further improve the accuracy of HDC encoding.

A. Inter-computing Processing: Revisiting a Sister Computing Paradigm, Stochastic Computing

SC has gained attention in recent years due to its intriguing advantages, including robustness to noise, high parallelism, and power efficiency [205], [207]. SC realizes complex arithmetic operations using simple logic gates, leading to significant cost savings in various applications such as image processing [208], sorting [209], and ML [210], [211]. In addition to surveying previous HDC research and underscoring the $\mathcal{H}\mathcal{V}$ mapping side, in this section, we discuss a new perspective towards new hypervector generation opportunities. We learn from the recent advancements of SC for generating high-quality correlated/unrelated bit-streams in generating HDC hypervectors. Table IV compares conventional computing (CC), SC, and HDC paradigms. CC involves positional binary radix representation and the concept of significant bits. SC and HDC enjoy holographic representations of binary data

with no significant digits. The atomic data in SC are bit-streams, while they are $\mathcal{H}\mathcal{V}$ s in HDC.

In HDC, the initial step is $\mathcal{H}\mathcal{V}$ mapping. There is no initial value generation in CC. Bit-stream or $\mathcal{H}\mathcal{V}$ assignment is an important step for SC and HDC. In SC, this assignment depends on logical comparison [142]. The encoding of any scalar value involves comparing the data value with some random numbers. For a bit-stream of length N , the input scalar (X) is compared with N random numbers (R). A ‘1’ is produced when $X > R$. A ‘0’ is produced, otherwise. In $\mathcal{H}\mathcal{V}$ generation, the initial encoding can be performed similarly for dense representation. In this respect, SC and HDC coincide. This method was used mainly when coding non-numeric symbols with orthogonal $\mathcal{H}\mathcal{V}$ s [2]. In HDC, the scalar value of X is a threshold value of 0.5 for all symbols (not to make a bias between 0 and 1 probability), and random $\mathcal{H}\mathcal{V}$ s are generated for different symbols (such as letters of an alphabet). The encoding step for HDC continues with multiply-add-permute operations; depending on the application, the steps may vary. In general, SC has a simpler and constant encoding procedure as it does not attribute holistic meaning to its bit-streams.

Compared to SC and CC, HDC has two concepts for storing data: item memory and associative memory. There is no different storage concept for CC and SC. In the scope of ML, the learning step is based on training the weights for CC. Here the weights can be a function parameter, polynomial coefficients, or NN coefficients. The resulting model is expressed in means of bit-streams in SC while stored as class $\mathcal{H}\mathcal{V}$ s in HDC. Class $\mathcal{H}\mathcal{V}$ s are cumulatively produced specifically for each class. Testing a model is based on the similarity comparison of the class $\mathcal{H}\mathcal{V}$ s and the test $\mathcal{H}\mathcal{V}$ in HDC. SC, on the other hand, can be thought of a paradigm where a similar structure in CC is expressed in the bit-stream domain only; SC offers an efficient solution in terms of hardware addressing the high complexity of CC designs (complex multipliers, full adders, etc.).

Although HDC has low model complexity, it is challenging in terms of accuracy and feature extraction. On the other hand, CC offers a high-accuracy model due to its precise representation. Considering the complexity, accuracy, and feature properties, SC lies between CC and HDC. In SC, the data is not vector symbolic; it is obtained by expressing scalar values directly with bit-streams. Categorical or symbolic data processing has not yet been a topic of SC (and it has a high potential for future work). The only issue is the built-in quantization property since SC is a discrete representation. Finally, SC and HDC provide a high fault tolerance [212], while CC is vulnerable to non-ideal hardware hazards and soft errors (i.e., bit flips).

B. Is Pseudo-randomization Really Needed?

In this section, we benchmark some important random sequences such as Sobol [142], Weyl (\bar{w}) [213], R2 (R) [214], Kasami (K) [215], Latin Hypercube (L) [216], Gold Code (G) [217], Hadamard (HD) [218], Faure (F) [219], Hammersly (HM) [220], Zadoff-Chu (Z) [221], Niederreiter (N) [222], [223], Poisson Disk (P) [224], and Van der Corput (VDC) [225] by answering the question “*Is pseudo-randomness can be replaced by quasi-randomness in HDC encoding?*”. The binary-valued sequences (logic-1 and logic-0), such as Kasami, Gold Code, and Hadamard, represent good orthogonality in terms of cosine similarity. The others involve the LD (quasi-random) property, which is defined as the measure of deviation from the uniformity [140]. The level of dynamicity varies depending on whether the same sequence is generated in each attempt of a generation process. Sequences such as Kasami, Latin Hypercube, Zadoff-Chu, and Poisson Disk exhibit dynamic behavior due to their pseudo-random properties. Fig. 2 displays several non-binary valued sequences, which include fixed- or floating-point numbers, along with their corresponding scattering plots. Each plot depicts two distinct sequences derived from each random number sequence listed above. We target $\mathcal{H}\mathcal{V}$ generation by using these random number sources.

The Weyl sequence is classified as an additive recurrence sequence, known for its generation through the iteration of

TABLE III
POPULATION OF PREVIOUS STUDIES CONSIDERING THE ENCODING FORMAT AND \mathcal{HV} SOURCE.

Previous Studies	Binding	Bundling	Perm ¹ .	RBF ²	RP ³	CA ⁴	tanh	CC ⁵	SC ⁶	ScC ⁷	DFT ⁸	KP ⁹	SKC ¹⁰ RAFE ¹¹	FQ ¹²	EELP ¹³	\mathcal{HV} Source ⁸
VoiceHD [19], AdaptHD [38], PRID [167], MIMHD [104], SemiHD [168], BinHD [73], QubitHD [127], QuantHD [35], HDCluster [21], HDC-IM [116], EnHDC [169], AdaptHD [38], TP-HDC [170], LeHDC [41], XCelHD [171], Multi-HDC [26], HyperRec [3], ScaleHD [9], HyperSpec [86], Imani et al. [24], Nazemi et al. [64], Montone et al. [94]	✓	✓	✗	✗	✗	✗	✗	✗	✗	✗	✗	✗	✗	✗	✗	Random
ST-HDC [106], RelHD [172], LookHD [173], GENERIC [92], BioHD [137], GraphHD [1], SHDC [174], HAM [175], Rahimi et al. [2], Datta et al. [148], Li et al. [11], Wu et al. [176], Karunaratne et al. [103], Rahimi et al. [55], [146], Kovalev et al. [93]	✓	✓	✓	✗	✗	✗	✗	✗	✗	✗	✗	✗	✗	✗	✗	Random
FebHD [161], DistHD [162], DUAL [105], NeuralHD [163], RE-FHDC [28], ManiHD [164], CascadeHD [177], SupportHD [178], TempHD [179], Yu et al. [29]	✗	✗	✗	✓	✗	✗	✗	✗	✗	✗	✗	✗	✗	✗	✗	Gaussian
SparseHD [180], F5-HD [150], compHD [181], HD-Core [182], HoloCN [165], Kleyko et al. [183], [89]	✗	✓	✓	✗	✗	✗	✗	✗	✗	✗	✗	✗	✗	✗	✗	Random
SecureHD [184], OnlineHD [143], SHEARer [166], FACH [185], SearchHD [72]	✓	✓	✗	✗	✗	✗	✗	✗	✗	✗	✗	✗	✗	✗	✗	Gaussian
PULP-HD [186], MHD [68], PerfHD [100], Schmuck et al. [152], Rahimi et al. [58], [54], Moin et al. [82]	✓✓*	✓	✓✓*	✗	✗	✗	✗	✗	✗	✗	✗	✗	✗	✗	✗	Random
ReHD [87], BRIC [71], HyperSpike [187], HDnn-PIM [32], HyDREA [101], FHDnn [188], FedHD [90], Prive-HD [124], THRIFTY [25], Gupta et al. [47], Morris et al. [189]	✗	✗	✗	✗	✓	✗	✗	✗	✗	✗	✗	✗	✗	✗	✗	Random
Laelaps [69], Burrello et al. [75], [74]	✓	✗	✗	✗	✗	✗	✗	✗	✗	✗	✗	✗	✗	✗	✗	LBP ¹⁴
GenieHD [135], Mitrokhin et al. [190], Rahimi et al. [10]	✓	✗	✓	✗	✗	✗	✗	✗	✗	✗	✗	✗	✗	✗	✗	Random
Menon et al. [191], [59]	✗	✗	✗	✗	✗	✓	✗	✗	✗	✗	✗	✗	✗	✗	✗	Random
HDNA [4]	✓	✓✓*	✓✓*	✗	✗	✓	✗	✗	✗	✗	✗	✗	✗	✗	✗	Random
Rosato et al. [192]	✓	✓	✗	✗	✗	✗	✗	✗	✗	✗	✗	✗	✗	✗	✗	TM ¹⁵ Code
Mitrokhin et al. [51]	✓	✗	✗	✗	✗	✗	✗	✗	✗	✗	✗	✗	✗	✗	✗	DH ¹⁶
Burrello et al. [81]	✓	✓	✗	✗	✗	✗	✗	✗	✗	✗	✗	✗	✗	✗	✗	LBP
tiny-HD [6]	✗	✗	✓	✗	✓	✗	✗	✗	✗	✗	✗	✗	✗	✗	✗	Random
Basaklar et al. [76]	✗	✓	✗	✗	✗	✗	✗	✗	✗	✗	✗	✗	✗	✗	✗	Random
Hersche et al. [84]	✗	✗	✗	✗	✓	✗	✗	✗	✗	✗	✗	✗	✗	✓	✓	Gaussian
Sutor et al. [52]	✗	✗	✗	✗	✗	✗	✓	✗	✗	✗	✗	✗	✗	✗	✗	NN output
Aygun et al. [129]	✓	✗	✓	✗	✗	✗	✗	✗	✗	✗	✗	✗	✗	✗	✗	LD-Seq.
Moghadam et al. [50]	✗	✓	✗	✗	✗	✗	✗	✗	✗	✗	✗	✗	✗	✗	✗	LD-Seq.
Chang et al. [56]	✓	✓	✗	✗	✗	✗	✗	✗	✗	✗	✗	✗	✗	✗	✗	Non-linear
HDCP [193]	✗	✗	✗	✗	✗	✗	✗	✓	✗	✗	✗	✗	✗	✗	✗	Random
StoCHD [102]	✗	✗	✗	✗	✗	✗	✗	✗	✓	✗	✗	✗	✗	✗	✗	Random
Rasanen [133]	✗	✗	✗	✗	✓	✗	✗	✗	✗	✓	✗	✗	✗	✗	✗	Non-linear
Kirilenco et al. [95]	✗	✗	✗	✗	✗	✗	✗	✗	✗	✗	✓	✗	✗	✗	✗	Gaussian
Xu et al. [194]	✗	✗	✗	✗	✗	✗	✗	✗	✗	✗	✗	✓	✗	✗	✗	Random
Hersche et al. [97]	✗	✗	✗	✗	✗	✗	✗	✗	✗	✗	✗	✗	✓	✗	✗	Gaussian

1:Permutation, 2: Radial Basis Function 3:Random Projection, 4:Cellular Automaton, 5:Circular Convolution, 6:Stochastic Computation, 7:Scatter Code, 8:Discrete Fourier Transform, 9:Kronecker Product, 10>Selective Kanerva Coding [195], 11: Randomized Activation Functions Encoding, 12:Feature Quantization, 13:End-to-End Learned Projection, 14: Local Binary Pattern [196], 15:Thermometer Code, 16:DeepHash [197]-[201].

*:The rows with ✓✓ mean the two-stage encoding approach. For instance the 6th row represents the methods incorporate *Binding* and *Bundling* operations at the first step and the *Binding* and *Permutation* operations at the second step.

⊛:The \mathcal{HV} source emphasizes the inherent process of generating the \mathcal{HV} .

TABLE IV
COMPARISON OF DIFFERENT COMPUTING PARADIGMS:
CONVENTIONAL BINARY COMPUTING, STOCHASTIC COMPUTING, AND HYPERDIMENSIONAL COMPUTING.

Computing Paradigm	Conventional Computing (CC)	Stochastic Computing (SC)	Hyperdimensional Computing (HDC)
Data Type	Bit	Bit-stream	Hypervector
Data Representation	Binary radix (most-, least-significant)	Unipolar, Bipolar, Likelihood Ratio, Inverted Bipolar	Binary, Bipolar, Sparse, Dense
Initial Encoding	No	Pseudo- or Quasi-random bit-streams	(Orthogonal) hypervectors
Encoding	2^n Bit Significant Encoding	Logical Comparison	Logical Multiply-Permute-Add
Storage	Memory	Memory	Item memory, Associative memory
ML Training	Weights	Weight Bit-streams	Class Hypervectors
Testing	Pre-trained classifier in binary format	Pre-trained classifier in bit-stream format	Pre-trained class hypervectors in hypervector format
Model Complexity	High	Low	Low
Feature Extraction	Easy	Moderate	Difficult

multiples of an irrational number modulo 1. Specifically, when considering $\beta \in \mathbb{R}$ as an irrational number and $b_i \in \{0, \beta, 2\beta, \dots, k\beta\}$, the sequence $b_i - \lfloor b_i \rfloor$ (b_i modulo 1) produces an equidistributed sequence within the interval (0, 1). Another example of an additive recurrence sequence is the R sequence, which is based on the *Plastic Constant*, a unique real solution of a cubic equation [214], [226]. In the case of Latin Hypercube sequences, the sampling space is divided into equally sized intervals, and a point within each interval is randomly selected [227].

The VDC sequence serves as the fundamental basis for many LD sequences. It is generated by reversing the digits of the corresponding base number and representing each integer value as a fraction within the interval [0, 1). For example, the decimal value 209 in base-7 is represented with $(416)_7$, and the corresponding value for the base-7 VDC sequence is $6 \times 7^{-1} + 1 \times 7^{-2} + 4 \times 7^{-3} = \frac{305}{343}$. Similarly, the Faure, Hammersley, and Halton sequences are derived from the concept of VDC using prime or co-prime numbers. To generate the Faure sequence in r -dimensions, the smallest prime number ω is chosen such that $\omega \geq r$. The first dimension of the Faure sequence corresponds to the VDC sequence with base- ω , while the remaining dimensions involve permutations of the first dimension. The q -dimensional Halton sequence is generated by utilizing the VDC sequence with different prime bases, starting from the first prime number to the q -th prime number. However, a limitation of the Halton sequence is the significant increase in the number of cycles required to adequately fill the q -dimensional hypercube in high dimensions [228]. The first Sobol sequence is based on the base-2 VDC sequence, while other Sobol sequences are generated through permutations of specific sets of direction vectors [204], [229]. The Niederreiter sequence is another variant of the VDC sequence that relies on the powers of prime numbers. This sequence incorporates irreducible and primitive polynomials to ensure LD and uniformity across the sample space [230]. The Poisson Disk sequence is a special kind of sampling method that generates evenly distributed samples with minimal distances between the points.

In order to evaluate the impact of LD sequences on the performance of HDC, we conducted a series of experiments involving image classification utilizing the widely-used MNIST dataset [39]. The encoding process considered both the pixel values for level \mathcal{HV} s and the pixel coordinates for position \mathcal{HV} s. Notably, each vector mapping was executed using a quasi-random LD sequence. For level \mathcal{HV} , the mapping was established based on a comparison between the sequence value and the corresponding numeric pixel value, allowing for the correlation of values in close proximity. On the other hand, for position \mathcal{HV} , the mapping was determined through the comparison between a constant threshold $Th=0.5$ and the sequence elements, thus ensuring orthogonality. Through this approach, we introduced a new and innovative method for 2D image encoding, showcasing the potential benefits of LD-sequences in HDC applications [50]. In Table V, we present the accuracy comparison for three distinct dimensions of $D=1K, 2K, \text{ and } 8K$. The final row in Table V highlights the utilization of random sequences (like in prior art) for generating the \mathcal{HV} s, with the average classification accuracy reported over 100 iterations.

The performance evaluation of the HDC architecture was

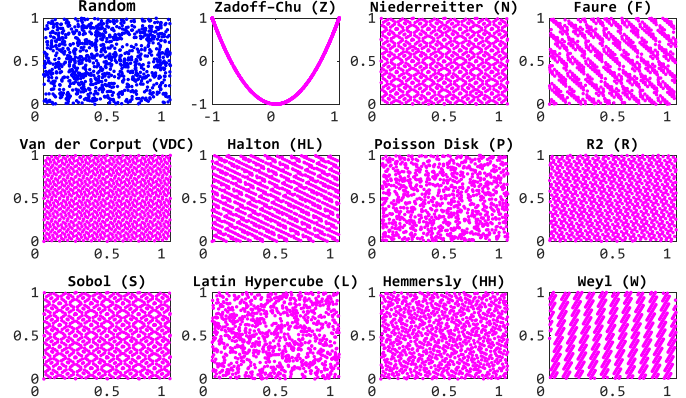


Fig. 2. The scatter plots of various sequences illustrate the distribution of each sequence in a 2D sample space consisting of 1024 points. The irrational numbers utilized for the Weyl sequence were π and the *Silver Ratio* ($\sqrt{2}-1$). The R2 sequence was generated using the *Plastic Constant*. For the Faure sequence, base-7 was employed. In the case of the Sobol sequence, the first two sequences from MATLAB's implementation of Sobol were utilized. The Halton sequence employed MATLAB's Halton implementation with bases 11 and 13. Bases 2 and 3 were utilized for the Hammersley sequence. The Zadorff-Chu sequence with a length of 1024 was created using MATLAB. Bases 2 and 1024 were used for the VDC sequence. The first two sequences of the Niederreiter sequence closely resembled the structure of the Sobol sequence, with permutations within the elements. The Poisson Disk sequence employed the minimal distances approach between points. Lastly, the Random sequence was generated using MATLAB's built-in `rand()` function.

conducted not only in terms of accuracy but also within the context of a NN-assisted system. For this purpose, a widely used convolutional neural network (CNN) architecture was initially employed, where HDC served as the classifier, and its accuracy performance was scrutinized. Additionally, in our prior work in [50], we took into account the potential accuracy challenges of HDC when applied to the CIFAR-10 dataset [49] without convolutional features, as highlighted by Dutta [32]. Table VI presents a comprehensive survey of the CIFAR-10 HDC system accuracy in previous works. The performance evaluation encompassed self-HDC (HDC as a standalone classifier), HDC integrated with CNN, and HDC aided by transfer learning, specifically utilizing the VGG11 architecture pre-trained on the ImageNet dataset. Remarkably, the proposed 2D image encoding scheme [50] exhibited improved accuracy performance for plain HDC, surpassing other SOTA designs in Table VI. Furthermore, the analysis conducted with CNN and transfer learning demonstrated enhanced accuracy performance compared to existing SOTA approaches. Additionally, the utilization of a combination of two different LD-sequences (such as Sobol+VDC), instead of one unique random source during vector mapping, has been harnessed to generate the \mathcal{HV} s, resulting in an improvement in the overall accuracy compared to the SOTA methods.

For the hardware efficiency, Table VII further compares the hardware cost of generating two \mathcal{HV} s of length $D = 256$. The comparison is performed for the Sobol, Halton and VDC sequences. The VDC sequence generator design utilizes a straightforward $\log_2 D$ -bit counter to generate sequence values for a specific base of D , assuming D is a power of 2. This design offers the advantage of simplicity and lightweight implementation, resulting in approximately $3.5\times$ and $9.58\times$

TABLE V
ACCURACY(%) COMPARISON OF MNIST DATASET FOR VARIOUS
LOW-DISCREPANCY SEQUENCES WITH DIFFERENT D SIZE.

LD-Seq.	$D=1K$	$D=2K$	$D=8K$
Sobol	85.13	86.37	87.28
Halton	53.45	66.44	82.65
Latin Hypercube	85.05	86.47	86.79
Niederreiter	76.08	77.64	77.70
Hammersley	53.44	66.77	82.87
Hadamard	83.68	83.95	84.19
Gold Code	78.52	78.84	78.94
Kasami	79.66	70.59	84.62
R2	85.73	85.98	87.18
Faure	61.51	77.45	85.77
Random	79.09	81.29	87.27

The evaluation for the Random case involved conducting 100 iterations, and the average classification accuracy was derived. LD-based $\mathcal{H}\mathcal{V}$ generation only needs 1 iteration.

TABLE VI
ACCURACY COMPARISON FOR CIFAR-10: SOTA HDCs vs. [50].

Method	Acc. (%)	Retrain	NN Assist.
SearHD (10K) [72] [41] [43]	22.66	No	No
BRIC (4K) [71] [32]	26.90	Yes	No
QuantHD (8K) [35] [41] [43]	28.42	Yes	No
LeHDC (10K) (BNN) [41]	46.10	Yes	Yes
Efficient HD (32) (BNN) [43]	46.18	Yes	Yes
GlueHD (8K) (Multiple NNs-MNNS) [52]	66.20	Yes	Yes
GlueHD (8K) (VGG11 + MNNS) [52]	90.80	Yes	Yes
Baseline HDC (10K) [41]	29.50	No	No
*Work in [50] with (8K) (Sobol + VDC)	42.72	No	No
*Work in [50] with (8K) (Halton + VDC)	34.72	No	No
*Work in [50] with (8K) (Sobol) (CNN [†])	53.62	No	Yes
*Work in [50] with (8K) (Halton) (CNN [†])	52.94	No	Yes
⊛Work in [50] with (8K) (Sobol) (VGG11)	90.97	Yes	Yes

*: plain-HDC, *: CNN[†] feature extraction assistance, ⊛: VGG-11 as a pre-trained model for transfer learning. †CNN uses three convolutional layers.

greater area efficiency compared to the Halton sequence generator and Sobol-based design, respectively. Moreover, in terms of power consumption, the VDC design demonstrates approximately $3.14\times$ and $1.53\times$ higher efficiency compared to the Halton and Sobol sequence designs, respectively. These findings highlight the favorable hardware characteristics of the VDC sequence generator, making it an attractive choice for $\mathcal{H}\mathcal{V}$ generation in practical implementations.

V. FROM CHALLENGES AND LIMITATIONS TO PROMISES AND RECOMMENDATIONS

In this section, we discuss the future prospects of HDC with a focus on the vector encoding step as the central theme of this survey. By examining previous works, we can gauge the potential promises and challenges associated with this emerging paradigm. The widespread adoption of HDC architectures in the next-generation of computing systems seems inevitable, with potential applications in (i) in-memory computing, (ii) flexible-printed electronics [231], (iii) quantum computing [62], and (iv) in-storage computing [47]. Notably, there already exist SOTA approaches for in-memory computing platforms [1], [11], [32], [47], [72], [101]–[116], where the fundamental operations of HDC can be easily implemented within the memory. However, one of the major challenges lies in generating high-quality $\mathcal{H}\mathcal{V}$ s while addressing the orthogonality and correlation issues.

Karunaratne et al. [103] discuss the possibility of implementing a complete HDC system on an in-memory computing (IMC) platform. They explore an N -gram-based encoding approach and similarity calculation through associative memory search, which operate exclusively in memory. On the other hand, Liu et al. propose an adapted method for Resistive Random-Access Memory (RRAM) devices for IMC in the HDC-IM framework [116]. In this framework, they propose some memory-based steps, such as bit-flipping, replication, shifting, and catenation, to generate item memory and continuous item memory, thereby offering a novel approach for handling the vector generation process in memory. However, future efforts related to in-memory $\mathcal{H}\mathcal{V}$ generation should also take into account the cost of each step, including shifting and catenation. Additionally, it is essential to numerically measure the degree of orthogonality after these steps to ensure the

TABLE VII
HARDWARE COST OF TWO HYPERVECTOR
GENERATIONS WITH $D = 256$ [50].

Seq.	Area (μm^2)	Power (μW)	Latency (ns)
Sobol	1562	24.64	0.68
Halton	580	50.45	1.06
VDC	163	16.05	0.49

The synthesized results were reported based on the Synopsys Design Compiler v2018.06 and the 45nm FreePDK gate library. The 2nd and 3rd sequences of the Sobol and base-2 and base-3 of the Halton sequence were used. For the VDC sequence case, any powers of 2-bases (e.g. 2,4,8,16,...) can be used.

quality of orthogonal $\mathcal{H}\mathcal{V}$ s achieved, thus presenting a new challenge for further research.

Speaking of bit-flipping, Basaklar et al. [76] discuss $\mathcal{H}\mathcal{V}$ design for edge devices in a broader context. They define a problem solution space for improving $\mathcal{H}\mathcal{V}$ design using a genetic algorithm. The D -dimensional level $\mathcal{H}\mathcal{V}$ s are represented using a quantized input space, and at each level, random bit-flipping (+1 \leftrightarrow -1) is applied to vector positions. The number of bit-flips at each level is treated as an optimization problem and solved using an evolutionary heuristic search approach. Nevertheless, it is crucial to acknowledge an important aspect overlooked in most prior-art works regarding $\mathcal{H}\mathcal{V}$ generation, which is the need for *lightweight* $\mathcal{H}\mathcal{V}$ designs. Particularly for IMC technologies, the limited operations might impact even polynomially-hard solutions for finding the best-performing $\mathcal{H}\mathcal{V}$ s. Thus, for the upcoming era of HDC research, emphasis should be placed on exploring on-device dynamic vector generation approaches that are lightweight and hardware-friendly.

Another promising avenue for future HDC research lies in custom processor design. Datta et al. [148] have taken the first step by proposing a 28nm Application-Specific Integrated Circuit (ASIC) processor architecture. This generic HD processor integrates multichannel sensor inputs and a $\mathcal{H}\mathcal{V}$ mapper, which facilitates vector generation into item and associative memory. The encoder is responsible for executing the necessary learning-based operations. However, to fully capitalize on the potential of HDC, there is a scope for exploring custom processor designs tailored to specific computer architectures. This could entail designing novel mnemonic codes, instructions, and customized data-flow to accommodate emerging HDC requirements. Particularly, for lightweight wearable sensing of biomedical data and classification tasks, a custom processor optimized for HDC could prove highly valuable. Notably, HDC has already demonstrated its effectiveness in various biomedical applications [58], [59], [69], [191]. In light of this, the development of specialized processors designed explicitly for HDC could lead to significant advancements in the field, enabling efficient and seamless integration of HDC-based solutions into wearable biomedical devices.

Another significant research direction with the potential to yield fruitful results is the exploration of the analogy between HDC systems and NNs. Ma and Jiao [42] have already provided valuable insights into this comparison by discussing the two learning strategies in a comparative manner. Notably, they highlight the effectiveness of NN-assisted HDC, which suggests that the generation of $\mathcal{H}\mathcal{V}$ s can be effectively managed using NN approaches. As a future prospect, researchers could investigate the possibility of replacing custom distributions with lightweight artificial intelligence methods for generating concise and efficient $\mathcal{H}\mathcal{V}$ s mapped to memory. Such an approach has the potential to become a prospective SOTA method. Duan et al. [41] have previously proclaimed HDC as a single-layer binarized neural network (BNN) architecture. They also discuss the limitations of the current HDC training trend. Two fundamental limitations are identified: (i) retraining in HDC differs from conventional NNs, as it only updates the misclassified class, leaving the true classes' $\mathcal{H}\mathcal{V}$ s unchanged. (ii) the retraining process in HDC is limited to a fixed step size when updating the class $\mathcal{H}\mathcal{V}$. Duan et al. point out that the derivative of loss, which is considered in conventional NNs, is overlooked in the HDC training system. Consequently, future studies could capitalize on this finding by integrating NNs and HDC, effectively merging

their principles into a unified approach. By leveraging the strengths of both HDC and NNs, researchers can potentially address the identified limitations and create a hybrid paradigm that offers enhanced learning capabilities and more efficient $\mathcal{H}\mathcal{V}$ generation techniques. This integration of HDC and NNs holds the promise of advancing the current SOTA in ML and memory-based computing, leading to novel applications and breakthroughs in various fields.

As we approach the conclusion of this survey, it is crucial to bring attention to a significant challenge that has been overlooked in the literature: the dynamic generation of $\mathcal{H}\mathcal{V}$ s during the encoding procedure in HDC systems. Most existing studies in HDC either rely on producing a seed vector and generating the remaining $\mathcal{H}\mathcal{V}$ s with a bit-flip technique [20], or they retrieve different randomly generated orthogonal vectors from memory units, such as look-up tables [173]. However, this raises an important issue: In scenarios involving online learning, where new data arrives continuously, a separate vector set is required for each new data instance. The dynamic generation of these new vector sequences becomes a key concern. In this regard, seeking support from other emerging computing technologies, such as SC may offer a promising research direction for HDC, fostering inter-computing collaboration between these emerging paradigms.

A recent study by Thomas et al. [232] addresses this dynamicity issue with an innovative hashing solution ([233]) for on-the-fly ([191]) vector generation, also known as *streaming encoding*. By revisiting and exploring inter-computing solutions, SC can serve as a valuable tool for streaming encoding, particularly due to its hardware-efficient nature. In SC, the hardware structure for bit-stream generation utilizes a simple generator comprising a linear-feedback shift register (LFSR) and a comparator [234]. This enables the production of correlated or uncorrelated sequences using the same or different LFSR modules, respectively, with ease [235]. It is worth noting that Chang et al. [170] have touched upon the possible utilization of a hardware-friendly LFSR approach in HDC systems. Nevertheless, further research is required in this domain, particularly exploring the potential of LD-sequences, as discussed in Section IV-B. In summary, the dynamic generation of $\mathcal{H}\mathcal{V}$ s during the encoding process presents a critical challenge for HDC systems, especially in scenarios involving online learning.

To sum up, we highly recommend the following future efforts as new research opportunities in the frame of HDC: ① streaming encoding and dynamic vector mapping for edge devices, ② study on biomedical applications of HDC frameworks (considering the populations of prior works reported in Table II), ③ new research efforts on the security and reliability side of the HDC systems (as Ma et al. [5] discuss), ④ similar to what we underscore in this work for SC, a high potential for collaborations between HDC and other emerging paradigms (such as neuromorphic computing), and ⑤ new HDC efforts for video processing.

VI. EXTRAS: AVAILABLE PLATFORMS AND SOTA SUMMARY

Additionally, we provide two concluding survey materials to facilitate a swift understanding of (i) readily available platforms and (ii) the prominent prior works that can serve as a source of inspiration for HDC researchers in refining the encoding procedure for their future endeavors.

Several open-source code projects on HDC have been released by various research groups. We list these prior releases in Table VIII. We assess the encoding methods showcased in each platform in this table. For instance, the developers of [236] have implemented random, level, thermometer, and circular $\mathcal{H}\mathcal{V}$ encoding in Python using PyTorch. Another open-source project, HD Torch [36], is also based on the PyTorch framework. HD Torch provides options for generating $\mathcal{H}\mathcal{V}$ s using the *random*, *sandwich*, *scale*, and *scale with radius* approaches. Here, the *sandwich* approach refers to encoding two neighboring vectors similarly for half of their elements and setting the remaining elements randomly. The *scale* method is an alternative term for level $\mathcal{H}\mathcal{V}$ generation,

TABLE VIII
PRIOR ARTS ON HDC IMPLEMENTATION WITH DIFFERENT PLATFORMS.

Project	Implementation (language percentage)	Encoding Details
TorchHD [236]	Python (100%)	random, level, thermometer, and circular $\mathcal{H}\mathcal{V}$ encoding
DistHD [162]	Python (100%)	Gaussian, RBF kernel
OpenHD [34]	Python, C++ (n.d.)	generic framework (a wrapper for GPU processing)
HD Torch [36]	Python (n.d.)	random, sandwich, scale, and scale with radius encoding
hdlib [237]	C (47.5%), Python (25.8%), CUDA (24.4%), Shell (2.3%)	random, <i>N-gram-based</i> encoding
Laelaps [69]	Python, CUDA, OpenMP (n.d.)	LBP Code [196]
PULP-HD [186]	C (98.8%), MATLAB (1.1%)	random, <i>Record-based + N-gram-based</i> encoding
VoiceHD [19]	Python (100%)	random binding bundling
MHD [68]	Python (100%)	random, <i>Record-based + N-gram-based</i>
PerfHD [100]	Python (100%)	random, <i>Record-based + N-gram-based</i>
HyperSpec [86]	Python (88.1%), Cython (8.7%), C++ (1.6%), Dockerfile (1.4%), Shell (0.2%)	random, <i>Record-based</i>
HDC Cluster [21]	Python (29.1%), Cuda (17.3%), C++ (38.7%), Makefile (13.2%), Shell (1.7%)	random, <i>Record-based</i>
PyBHV [238]	Python (65.9%), C++ (25.6%), C (8.5%)	random
HD Classification [239]	C++ (43.1%), Cuda (25.5%), Python (13.4%), Makefile (12.9%), Shell (5.1%)	random
constrained FSCIL [240]	Python (100%)	quasi-random vector generation for uncorrelation
HDC Language Recognition [2]	MATLAB, Verilog (n.d.)	dense bipolar $\mathcal{H}\mathcal{V}$ encoding
Dynamic Vision Sensor with HDC [97]	C (49.8%), Python (12.4%), Objective-C (36.6%)	selective Kanerva coding [195], Randomized Activation Function
HDC-MER [56]	MATLAB (100%)	random non-linear function
EMG-based gesture recognition [82], Hand gesture recognition [58]	MATLAB (100%)	random, <i>Record-based + N-gram-based</i>
On-chip learning HDC library [152]	VHDL (91.8%), MATLAB (8.2%)	random, <i>Record-based + N-gram-based</i>
HD embedding-BCI [84]	Python (100%)	random projection feature quantization learned projection
HDC-EEG-ERP [55]	MATLAB (100%)	random binding bundling permutation
HD pattern recognition [89]	MATLAB (100%)	random bundling permutation
HDC Parallel Single-pass Learning [29]	Python (100%)	Gaussian, RBF kernel

n.d.: not defined.

TABLE IX
SUMMARY OF NOTICEABLE SOTA WORKS HIGHLIGHTING APPLICATIONS, \mathcal{HV} MAPPING, AND HARDWARE.

Year, Authors	Contribution	Application, Dataset (Accuracy, D)	Vector Generation & Encoding Details	Environment, Model, or Hardware Details	Hardware Efficiency
2018, Imani et al. ♠ [68]	Decreasing classification cost	Speech recognition ISOLET (95.9%, $D=10,000$)	Random-Bipolar \mathcal{HV} Bit-flipping applied Hierarchical multi-encoder: I. Record-based II. N-gram-based	Synopsys Design Compiler (TSMC 45nm)	Energy (6.6×) Speed (6.3×)
♠ [68] Imani et al. target reducing the classification cost by inspecting the reduced \mathcal{HV} size. To achieve this problem, they use a multi-encoder strategy to best select the proper encoder between record-based or N-gram-based encoding approaches. The vector generation details on hardware are not shared, and random generation via nearly orthogonal vectors is generated with bit-flipping. The bipolar structure is utilized.					
2020, Nazemi et al. ♦ [64]	Automatic feature extraction	Activity Recognition HAR (96.44%, $D=10,240$) Speech Recognition ISOLET (96.67%, $D=10,240$)	Random seed \mathcal{HV} Bit-flipping Binding and Bundling	FPGA (Xilinx UltraScale+ VU9P)	BRAMs (1.8%) DSPs (15%) FFs (0.8%) LUTs (5.1%) Latency (23.3 us) Power (5.3 W)
♦ [64] Nazemi et al. target the automated feature extraction using NNs that feed an HDC system. They use hard-wired features and LUT-based levels driven by the DRAM module. The work leads to the idea of an NN-assisted HDC system; however, dependency on an NN system for full-independent on-edge training efforts might be further discussed.					
2018, Wu et al. ✨ [10]	Exploring the opportunities of HDC for next generation devices (nanotubes, RRAM)	21 European languages classification Europarl (98%)	Evenly spaced time-delay encoding	Synopsys Design Compiler CNFET and RRAM-based design	# of CNFET (1952) # of RRAM (224)
✨ [10] Wu et al. explore the HDC's novel capacity for emerging device platforms such as nanotubes. The very interesting side of this work lies in the area of solid-state circuits; they present a CNFET (carbon nanotube field-effect transistor) and RRAM-based random projection unit for vector mapping, which is one of its kind. Further design efforts following the same procedures in-memory computing platforms may yield fruitful outcomes.					
2021, Zou et al. ♣ [164]	Adaptive encoder and non-linear interactions between the features during the encoding	Digit recognition MNIST (>97%) Power prediction PECAN (>97%) Voice recognition ISOLET (>95%) Activity recognition UCIHAR (>98%) Position recognition EXTRA (>84%) ($D = 4,000$ for all)	Manifold-selection-based encoding Gaussian distribution for initial vectors	In software: C++ In hardware: FPGA (Kintex-7)	12.3× speed-up 19.3× energy-efficiency
♣ [164] Zou et al. propose an adaptive encoder that performs non-linear interactions between the features. This work is a leading work that addresses the static encoder to make an adaptive one. Thus, maximum learning accuracy is targeted. Another important aspect of this work is the real-time data encoding and learning property. This is quite important for streaming data and a dynamic learning platform. An unsupervised manifold technique is utilized during the vector generation; the Gaussian distribution-based random \mathcal{HV} s are multiplied by the manifold to obtain an adaptive HD encoder. This work proposes to reduce the D size from 10,000 to 4,000 for the same amount of accuracy.					
2015, Räsänen ★ [133]	Vector generation for non-discrete data	Spoken word classification CAREGIVER Y2 UK corpus > 97%, $D=4,000$	S-WARP Mapping and Weighted Accumulation of Random Projections	No information given	No hardware implementation
★ [133] Räsänen et al. propose a way to generate \mathcal{HV} s holding local similarities in the input vectors by setting generalization toward new inputs. The encoding procedure guarantees mapping quasi-orthogonal vectors for distant inputs. Features from raw data (e.g., mel-frequency from speech data) are utilized to transform them into the hyperspace. The Weighted Accumulation of Random Projections (WARP) method and scatter code are utilized for feature mapping that guides the generation of \mathcal{HV} s. The proposed method brings interesting ideas for the continuous data from the sensory inputs. However, more of the hardware implementability must be discussed, considering the current load of the proposal to the hardware platform.					
2019, Chang et al. ✨ [56]	\mathcal{HV} embedding using random non-linearity	Galvanic Skin Response, Electroencephalogram, Electrocardiogram dataset (AMIGOS) binary emotion classification (76.6%, $D=10,000$)	Multiplexer-based ternary (-1, 0, +1) feature mapping into hyperspace	No information given	Only system block diagram is given
✨ [56] Chang et al. use lightweight design for the embedding of vectors using multiplexers. The generation step is degraded into a simple operation using the sign of the biomedical feature for the selection port of the multiplexer. Multi-modal sensor data are mapped into holistic representations.					
2020, Kim et al. ★ [135]	DNA representation in high dimensional \mathcal{HV} s and accelerated pattern match	DNA Pattern Matching *Escherichia coli *Human chromosome14 *Random sequence (>99.99%, $D=100,000$)	Random-Bipolar base \mathcal{HV} s Shifting and multiplication-based encoding	GPU (NVIDIA GTX 1080 Ti) and FPGA (Kintex-7 KC705)	44.4× speedup 54.1× energy-efficiency on FPGA
★ [135] Kim et al. propose chunk-processing of very long \mathcal{HV} s targeted to represent holistic nucleoid representations in DNA sequences. The idea behind this work is to parallelize the operations, especially for ultra-long \mathcal{HV} s. The vector generations are not based on any specific hardware design, and only just approximate random generations are utilized. It is important to note that for applications requiring low-count symbols like DNA (Adenine, Guanine, Cytosine, and Thymine), the number of the generated base \mathcal{HV} s is limited; it does not necessarily base on the dynamic vector generation. This work is also one of its kind that process vector size up to 100,000 ultra-long dimensions.					
2019, Liu et al. ✨ [116]	RRAM-based HDC in-memory architecture	Voice recognition ISOLET (92.1%, $D=8,192$)	Block generation of \mathcal{HV} s on crossbar XOR-summation encoding	RRAM, CPU, and GPU separately	2.28 J Energy in-memory 3960 J Energy CPU
✨ [116] Liu et al. introduce a modified technique for RRAM devices considering IMC. The proposed framework suggests a unique approach involving memory-based bit-flipping, replication, shifting, and catenation steps to generate both item memory and continuous item memory. Their innovative method presents a fresh perspective on handling vector generations within the memory.					

while *scale with radius* utilizes a distance parameter called radius to encode vectors proportionally based on their distance closer than the radius [69].

Kang et al. [34] propose OpenHD, an abstract framework designed for GPU-powered operations. Their framework enables designers to implement an initial Python code and then utilize the HD decorator to obtain a GPU-accelerated version via Just-In-Time (JIT) compilation [70], [171]. The *Semantic Vectors Package* in [241] supports dense and sparse random vector encoding for concept-aware knowledge representation tasks in natural language processing. This package is implemented in both Java and Python. The *hdlib* repository [237] is an open-source code project that offers *N-gram-based* vector symbolic classification and includes CPU and GPU-based optimizations. Additionally, a PyTorch implementation targeting few-shot learning with a combination of HDC systems and NNs is available in [242]. This repository employs quasi-random encoding for image data to obtain uncorrelated vectors [240]. We highly recommend exploring the rest of the platforms for further investigation and insights.

Finally, it is essential to highlight a summary of remarkable SOTA works in the literature which have made significant contributions to vector mapping and encoding. Table IX provides a comprehensive overview of these works, and the accompanying details encompass various aspects, ranging from dataset utilization to hardware efficiency. Each entry includes summary notes pertaining to the overall encoding approach and noteworthy observations.

VII. CONCLUSIONS

This study delves into a comprehensive exploration of hypervector encoding, the primary and pivotal stage in Hyperdimensional Computing (HDC), utilizing various methods and techniques, with a particular focus on the hypervector generation phase. Despite the promising potentials of HDC, there has been a relatively limited study on the critical step of data generation, known as the initial hypervector encoding. This encoding process plays a fundamental role in the architecture design and accuracy of HDC systems. Prior state-of-the-art research has primarily emphasized the holistic structure of HDC, leaving less exploration of the promising potential for conducting computations across paradigms, including stochastic computing (SC), during the hypervector generation, also referred to as initial vector mapping. In this study, we addressed this gap by providing an in-depth literature analysis of HDC and introducing readers to a novel perspective on initial vector mapping. Through an in-depth exploration of the interplay between SC and HDC, we emphasize their effectiveness, highlighting the significance of this research in advancing the field. Our aim is to contribute to a better understanding and utilization of these computational approaches, thereby fostering further progress in the HDC domain.

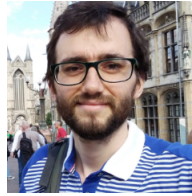
REFERENCES

- [1] P. Poduval et al. Graphd: Graph-based hyperdimensional memorization for brain-like cognitive learning. *Frontiers in Neuroscience*, 16, 2022.
- [2] A. Rahimi et al. A robust and energy-efficient classifier using brain-inspired hyperdimensional computing. In *ISLPED*, ISLPED '16, pp. 64–69, 2016.
- [3] Y. Guo et al. Hyperrec: Efficient recommender systems with hyperdimensional computing. In *ASP-DAC*, ASPDAC'21, pp. 384–389, 2021.
- [4] M. Imani et al. Hdna: Energy-efficient dna sequencing using hyperdimensional computing. In *IEEE EMBS International Conference BHI*, pp. 271–274, 2018.
- [5] D. Ma et al. Robust hyperdimensional computing against cyber attacks and hardware errors: A survey. In *ASP-DAC*, pp. 598–605, 2023.
- [6] B. Khaleghi et al. tiny-hd: Ultra-efficient hyperdimensional computing engine for iot applications. In *DATE*, pp. 408–413, 2021.
- [7] P. Stanley-Marbell et al. Exploiting errors for efficiency: A survey from circuits to applications. *ACM Comput. Surv.*, 53(3), jun 2020.
- [8] A. Alaghi et al. The promise and challenge of stochastic computing. *IEEE TCAD*, 37(8):1515–1531, 2018.
- [9] S. Zhang et al. Scalehd: Robust brain-inspired hyperdimensional computing via adaptive scaling. In *ICCAD*, pp. 1–9, 2022.
- [10] T. F. Wu et al. Hyperdimensional computing exploiting carbon nanotube fets, resistive ram, and their monolithic 3d integration. *IEEE JSSC*, 53(11):3183–3196, 2018.
- [11] H. Li et al. Hyperdimensional computing with 3d vrram in-memory kernels: Device-architecture co-design for energy-efficient, error-resilient language recognition. In *IEEE IEDM*, pp. 16.1.1–16.1.4, 2016.
- [12] C.-Y. Chang et al. Recent progress and development of hyperdimensional computing (hdc) for edge intelligence. *IEEE JESTCS*, 13(1):119–136, 2023.
- [13] D. Kleyko et al. A survey on hyperdimensional computing aka vector symbolic architectures, part ii: Applications, cognitive models, and challenges. *ACM Comput. Surv.*, 55(9), jan 2023.
- [14] D. Kleyko et al. A survey on hyperdimensional computing aka vector symbolic architectures, part i. *ACM Comput. Surv.*, 55(6), 2022.
- [15] E. Hassan et al. Hyper-dimensional computing challenges and opportunities for ai applications. *IEEE Access*, 10:97651–97664, 2022.
- [16] L. Ge and K. K. Parhi. Classification using hyperdimensional computing: A review. *IEEE Circ. and Syst. Mag.*, 20(2):30–47, 2020.
- [17] V. GRITSENKO et al. Neural autoassociative memories for binary vectors: A survey, Jun 2017.
- [18] A. X. Manabat et al. Performance analysis of hyperdimensional computing for character recognition. In *ISMAC*, pp. 1–5, 2019.
- [19] M. Imani et al. Voicehd: Hyperdimensional computing for efficient speech recognition. In *IEEE ICRC*, pp. 1–8, 2017.
- [20] Z. Zou et al. EventHD: Robust and efficient hyperdimensional learning with neuromorphic sensor. *Frontiers in Neuroscience*, 16, July 2022.
- [21] M. Imani et al. Hdcluster: An accurate clustering using brain-inspired high-dimensional computing. In *DATE*, pp. 1591–1594, 2019.
- [22] J. Reyes et al. Human Activity Recognition Using Smartphones. UCI Machine Learning Repository, 2012. DOI: <https://doi.org/10.24432/C54S4K>.
- [23] L. Smets et al. Training a hyperdimensional computing classifier using a threshold on its confidence, 2023.
- [24] Y. Kim et al. Efficient human activity recognition using hyperdimensional computing. In *Proceedings of the 8th International Conference on the Internet of Things, IOT '18*, 2018.
- [25] S. Gupta et al. Thrifty: Training with hyperdimensional computing across flash hierarchy. In *ICCAD*, pp. 1–9, 2020.
- [26] C.-Y. Chang et al. Multa-hdc: A multi-task learning framework for hyperdimensional computing. *IEEE TComp.*, 70(8):1269–1284, 2021.
- [27] Y.-R. Hsiao et al. Hyperdimensional computing with learnable projection for user adaptation framework. In *AIAI*, pp. 436–447, Cham, 2021.
- [28] N. Zeulin et al. Resource-efficient federated hyperdimensional computing, 2023.
- [29] T. Yu et al. Understanding hyperdimensional computing for parallel single-pass learning. In *ANIPS*, volume 35, pp. 1157–1169. Curran Associates, Inc., 2022.
- [30] R. Cole and M. Fenty. ISOLET. UCI Machine Learning Repository, 1994. DOI: <https://doi.org/10.24432/C51G69>.
- [31] A. Kazemi et al. Achieving software-equivalent accuracy for hyperdimensional computing with ferroelectric-based in-memory computing. *Scientific Reports*, 12(1):19201, Nov 2022.
- [32] A. Duita et al. Hdnn-pim: Efficient in memory design of hyperdimensional computing with feature extraction. In *GLSVLSI'22*, pp. 281–286, 2022.
- [33] A. Reiss. PAMAP2 Physical Activity Monitoring. UCI Machine Learning Repository, 2012. DOI: <https://doi.org/10.24432/C5NW2H>.
- [34] J. Kang and Y. Kim. hyperdimensional-computing. <https://github.com/UCSD-SEELab/openhd>, 2022. date accessed: 01-21-2023.
- [35] M. Imani et al. Quanthd: A quantization framework for hyperdimensional computing. *IEEE TCAD*, 39(10):2268–2278, 2020.
- [36] W. A. Simon et al. Hdtorch: Accelerating hyperdimensional computing with gp-gpus for design space exploration. In *ICCAD*, 2022.
- [37] G. Griffin et al. Caltech 256, Apr 2022.
- [38] M. Imani et al. Adapthd: Adaptive efficient training for brain-inspired hyperdimensional computing. In *BioCAS*, pp. 1–4, 2019.
- [39] Y. Lecun et al. Gradient-based learning applied to document recognition. *Proceedings of the IEEE*, 86(11):2278–2324, 1998.
- [40] Y.-C. Chuang et al. Dynamic hyperdimensional computing for improving accuracy-energy efficiency trade-offs. In *IEEE Workshop on SiPS*, pp. 1–5, 2020.
- [41] S. Duan et al. Lehdc: Learning-based hyperdimensional computing classifier. *DAC'22*, pp. 1111–1116, 2022.
- [42] D. Ma and X. Jiao. Hyperdimensional computing vs. neural networks: Comparing architecture and learning process, 2022.
- [43] Zhanglu Yan et al. Efficient hyperdimensional computing, 2023. 2301.10902 arXiv.
- [44] S. Duan et al. A brain-inspired low-dimensional computing classifier for inference on tiny devices, 2022.
- [45] V. Miranda and O. d'Aliberti. Hyperdimensional computing encoding schemes for improved image classification. In *IEEE ISTHS*, pp. 1–9, 2022.
- [46] D. Campos and J. Bernardes. Cardiotocography. UCI Machine Learning Repository, 2010. DOI: <https://doi.org/10.24432/C51S4N>.
- [47] S. Gupta et al. Store-n-learn: Classification and clustering with hyperdimensional computing across flash hierarchy. *ACM Trans. Embed. Comput. Syst.*, 21(3), jul 2022.
- [48] S. Thomann et al. Hw/sw co-design for reliable team-based in-memory brain-inspired hyperdimensional computing. *IEEE TComp*, 72(8):2404–2417, 2023.
- [49] A. Krizhevsky. Learning multiple layers of features from tiny images. 2009.
- [50] M. Shoushtari Moghadam et al. No-multiplication deterministic hyperdimensional encoding for resource-constrained devices. *IEEE Embedded Systems Letters*, 2023. In-press.
- [51] A. Mitrokhin et al. Symbolic representation and learning with hyperdimensional computing. *Frontiers in Robotics and AI*, 7, 2020.
- [52] Peter Sutor et al. Gluing neural networks symbolically through hyperdimensional computing, 2022. 2205.15534 arXiv.
- [53] U. Pale et al. Multi-centroid hyperdimensional computing approach for epileptic seizure detection. *Frontiers in Neurology*, 13, 2022.

- [54] A. Rahimi *et al.* Efficient biosignal processing using hyperdimensional computing: Network templates for combined learning and classification of exg signals. *Proceedings of the IEEE*, 107(1):123–143, 2019.
- [55] A. Rahimi *et al.* Hyperdimensional computing for blind and one-shot classification of eeg error-related potentials. *Mob. Neww. Appl.*, 25(5):1958–1969, oct 2020.
- [56] E.-J. Chang *et al.* Hyperdimensional computing-based multimodality emotion recognition with physiological signals. In *AICAS*, pp. 137–141, 2019.
- [57] K. A. Schindler and A. Rahimi. A primer on hyperdimensional computing for ieeg seizure detection. *Frontiers in Neurology*, 12, 2021.
- [58] A. Rahimi *et al.* Hyperdimensional biosignal processing: A case study for emg-based hand gesture recognition. In *IEEE ICRC*, pp. 1–8, 2016.
- [59] A. Menon *et al.* Efficient emotion recognition using hyperdimensional computing with combinatorial channel encoding and cellular automata. *Brain Informatics*, 9(1):14, Jun 2022.
- [60] M. Laiho *et al.* High-dimensional computing with sparse vectors. In *BioCAS*, pp. 1–4, 2015.
- [61] T. Plate. Holographic reduced representations. *IEEE TNN*, 6(3):623–641, 1995.
- [62] D. Aerts *et al.* Geometric analogue of holographic reduced representation. *Journal of Mathematical Psychology*, 53(5):389–398, 2009. Special Issue: Quantum Cognition.
- [63] J. Snider and S. Franklin. Modular composite representation. *Cognitive Computation*, 6(3):510–527, Sep 2014.
- [64] M. Nazemi *et al.* Synergiclearning: Neural network-based feature extraction for highly-accurate hyperdimensional learning. In *ICCAD*, ICCAD’20, 2020.
- [65] P. Kanerva. Hyperdimensional computing: An introduction to computing in distributed representation with high-dimensional random vectors. *Cognitive Computation*, 1(2):139–159, Jun 2009.
- [66] P. Kanerva. Computing with high-dimensional vectors. *IEEE Design & Test*, 36(3):7–14, 2019.
- [67] P. Neubert *et al.* An introduction to hyperdimensional computing for robotics. *KI - Künstliche Intelligenz*, 33(4):319–330, Dec 2019.
- [68] M. Imani *et al.* Hierarchical hyperdimensional computing for energy efficient classification. In *DAC*, pp. 1–6, 2018.
- [69] A. Burrello *et al.* Laelaps: An energy-efficient seizure detection algorithm from long-term human ieeg recordings without false alarms. In *DATE*, pp. 752–757, 2019.
- [70] J. Kang *et al.* Openhd: A gpu-powered framework for hyperdimensional computing. *IEEE TComp*, 2022.
- [71] M. Imani *et al.* Bric: Locality-based encoding for energy-efficient brain-inspired hyperdimensional computing. In *DAC*, pp. 1–6, 2019.
- [72] M. Imani *et al.* Searchd: A memory-centric hyperdimensional computing with stochastic training. *IEEE TCAD*, 39(10):2422–2433, 2020.
- [73] M. Imani *et al.* A binary learning framework for hyperdimensional computing. In *2019 DATE*, pp. 126–131, 2019.
- [74] A. Burrello *et al.* Hyperdimensional computing with local binary patterns: One-shot learning of seizure onset and identification of ictogenic brain regions using short-time ieeg recordings. *IEEE Transactions on Biom. Eng.*, 67(2):601–613, 2020.
- [75] A. Burrello *et al.* One-shot learning for ieeg seizure detection using end-to-end binary operations: Local binary patterns with hyperdimensional computing. In *BioCAS*, pp. 1–4, 2018.
- [76] T. Basaklar *et al.* Hypervector design for efficient hyperdimensional computing on edge devices, 2021.
- [77] A. Menon *et al.* Brain-inspired multi-level control of an assistive prosthetic hand through emg task recognition. In *BioCAS*, pp. 384–388, 2022.
- [78] J. Morris *et al.* Adaptbit-hd: Adaptive model bitwidth for hyperdimensional computing. In *ICCD*, pp. 93–100, 2021.
- [79] L. Ge and K. K. Parhi. Seizure detection using power spectral density via hyperdimensional computing. In *IEEE ICASSP*, pp. 7858–7862, 2021.
- [80] F. Asgarinejad *et al.* Detection of epileptic seizures from surface eeg using hyperdimensional computing. In *42nd Annual International Conference of the IEEE EMBC*, pp. 536–540, 2020.
- [81] A. Burrello *et al.* One-shot learning for ieeg seizure detection using end-to-end binary operations: Local binary patterns with hyperdimensional computing. In *BioCAS*, pp. 475 – 478, 2018.
- [82] A. Moin *et al.* An emg gesture recognition system with flexible high-density sensors and brain-inspired high-dimensional classifier. In *ISCAS*, pp. 1–5, 2018.
- [83] N. Watkinson *et al.* Detecting COVID-19 related pneumonia on CT scans using hyperdimensional computing. *Annu Int Conf IEEE Eng Med Biol Soc*, 2021:3970–3973, November 2021.
- [84] M. Hersche *et al.* Exploring embedding methods in binary hyperdimensional computing: A case study for motor-imagery based brain-computer interfaces. December 2018.
- [85] D. Kleyko *et al.* A hyperdimensional computing framework for analysis of cardiorespiratory synchronization during paced deep breathing. *IEEE Access*, 7:34403–34415, 2019.
- [86] W. Xu *et al.* Hyperspec: Ultrafast mass spectra clustering in hyperdimensional space. *Journal of Proteome Research*, 2023.
- [87] J. Morris *et al.* Locality-based encoder and model quantization for efficient hyper-dimensional computing. *IEEE TCAD*, 41(4):897–907, 2022.
- [88] D. Ma *et al.* Testing and enhancing adversarial robustness of hyperdimensional computing. *IEEE TCAD*, pp. 1–1, 2023.
- [89] D. Kleyko *et al.* Classification and recall with binary hyperdimensional computing: Tradeoffs in choice of density and mapping characteristics. *IEEE TNNLS*, 29(12):5880–5898, 2018.
- [90] Q. Zhao *et al.* Fedhd: Federated learning with hyperdimensional computing. In *MobiCom*, pp. 791–793, 2022.
- [91] M. Yasser *et al.* An efficient hyperdimensional computing paradigm for face recognition. *IEEE Access*, 10:85170–85179, 2022.
- [92] B. Khaleghi *et al.* Generic: Highly efficient learning engine on edge using hyperdimensional computing. In *DAC*, DAC’22, pp. 1117–1122, 2022.
- [93] A. K. Kovalev *et al.* Vector semiotic model for visual question answering. *Cognitive Systems Research*, 71:52–63, 2022.
- [94] G. Montone *et al.* Hyper-dimensional computing for a visual question-answering system that is trainable end-to-end, 2017.
- [95] D. E. Kirilenko *et al.* Question answering for visual navigation in human-centered environments. In *Advances in Soft Computing*, 2021.
- [96] P. R. Gensler and H. Amrouch. Brain-inspired computing for wafer map defect pattern classification. In *2021 IEEE International Test Conference (ITC)*, pp. 123–132, 2021.
- [97] M. Hersche *et al.* Integrating event-based dynamic vision sensors with sparse hyperdimensional computing: A low-power accelerator with online learning capability. In *ISLPED*, ISLPED ’20, pp. 169–174, 2020.
- [98] N. Anwar *et al.* Towards an improved hyperdimensional classifier for event-based data. In *2023 57th Annual Conference on Information Sciences and Systems (CISS)*, pp. 1–4, 2023.
- [99] M. Bettayeb *et al.* Spatialhd: Spatial transformer fused with hyperdimensional computing for ai applications. In *AICAS*, pp. 1–5, 2023.
- [100] D. Ma *et al.* Perhd: Efficient vit architecture performance ranking using hyperdimensional computing. In *Proceedings of the IEEE/CVF Conference on Computer Vision and Pattern Recognition (CVPR) Workshops*, pp. 2229–2236, June 2023.
- [101] J. Morris *et al.* Hydrea: Utilizing hyperdimensional computing for a more robust and efficient machine learning system. *ACM Trans. Embed. Comput. Syst.*, 21(6), oct 2022.
- [102] P. Poduval *et al.* Stochd: Stochastic hyperdimensional system for efficient and robust learning from raw data. In *2021 DAC*, pp. 1195–1200, 2021.
- [103] G. Karunaratne *et al.* In-memory hyperdimensional computing. *Nature Electronics*, 3(6):327–337, Jun 2020.
- [104] A. Kazemi *et al.* Mimhd: Accurate and efficient hyperdimensional inference using multi-bit in-memory computing. In *ISLPED*, pp. 1–6, 2021.
- [105] M. Imani *et al.* Dual: Acceleration of clustering algorithms using digital-based processing in-memory. In *MICRO*, pp. 356–371, 2020.
- [106] G. Karunaratne *et al.* Energy efficient in-memory hyperdimensional encoding for spatio-temporal signal processing. *IEEE TCAS II*, 68(5):1725–1729, 2021.
- [107] P. Poduval *et al.* Robust in-memory computing with hyperdimensional stochastic representation. In *NANOARCH*, pp. 1–6, 2021.
- [108] G. Karunaratne *et al.* Robust high-dimensional memory-augmented neural networks. *Nature Communications*, 12, 2020.
- [109] J. Langenegger *et al.* In-memory factorization of holographic perceptual representations. *Nature Nanotechnology*, 18(5):479–485, May 2023.
- [110] R. Guirado *et al.* Whype: A scale-out architecture with wireless over-the-air majority for scalable in-memory hyperdimensional computing. *IEEE JESTCS*, 13(1):137–149, 2023.
- [111] G. Karunaratne *et al.* In-memory realization of in-situ few-shot continual learning with a dynamically evolving explicit memory. In *ESSCIRC*, pp. 105–108, 2022.
- [112] R. Guirado *et al.* Wireless on-chip communications for scalable in-memory hyperdimensional computing. In *IJCNN*, pp. 1–8, 2022.
- [113] S. Thomann *et al.* All-in-memory brain-inspired computing using FeFET synapses. *Frontiers in Electronics*, 3, February 2022.
- [114] J. Cai *et al.* Hyperlock: In-memory hyperdimensional encryption in memristor crossbar array, 2022.
- [115] L. Yang *et al.* Self-selective memristor-enabled in-memory search for highly efficient data mining. *InfoMat*, 5(5):e12416, 2023.
- [116] J. Liu *et al.* Hdc-im: Hyperdimensional computing in-memory architecture based on rram. In *2019 26th IEEE International Conference on Electronics, Circuits and Systems (ICECS)*, pp. 450–453, 2019.
- [117] H. Amrouch *et al.* Brain-inspired hyperdimensional computing for ultra-efficient edge ai. In *2022 CODES+ISSS*, 2022.
- [118] F. Yang and S. Ren. On the vulnerability of hyperdimensional computing-based classifiers to adversarial attacks. In *Network and System Security: 14th International Conference, NSS 2020, Melbourne, VIC, Australia, November 25–27, 2020, Proceedings*, pp. 371–387, Berlin, Heidelberg, 2020. Springer-Verlag.
- [119] H. Moraliyage *et al.* Evaluating the adversarial robustness of text classifiers in hyperdimensional computing. In *2022 15th International Conference on Human System Interaction (HSI)*, pp. 1–8, 2022.
- [120] O. Gungor *et al.* Res-hd: Resilient intelligent fault diagnosis against adversarial attacks using hyper-dimensional computing, 2022.
- [121] O. Gungor *et al.* Adversarial-hd: Hyperdimensional computing adversarial attack design for secure industrial internet of things. In *Proceedings of Cyber-Physical Systems and Internet of Things Week 2023, CPS-IoT Week ’23*, pp. 1–6, 2023.
- [122] J. Wang *et al.* Late breaking results: Scalable and efficient hyperdimensional computing for network intrusion detection, 2023.
- [123] M. Hersche *et al.* Evolvable hyperdimensional computing: Unsupervised regeneration of associative memory to recover faulty components. In *AICAS*, pp. 281–285, 2020.
- [124] B. Khaleghi *et al.* Prive-hd: Privacy-preserved hyperdimensional computing. In *DAC*, pp. 1–6, 2020.
- [125] F. Yang and S. Ren. Adversarial attacks on brain-inspired hyperdimensional computing-based classifiers, 2020.
- [126] X. Wang *et al.* Real-time detection of electrical load anomalies through hyperdimensional computing. *Energy*, 261:125042, 2022.
- [127] S. Bosch *et al.* Qubithd: A stochastic acceleration method for hd computing-based machine learning. *ArXiv*, abs/1911.12446, 2019.
- [128] Y. Hao *et al.* Stochastic-hd: Leveraging stochastic computing on hyperdimensional computing. In *ICCD*, pp. 321–325, 2021.

- [129] S. Aygun *et al.* A linear-time, optimization-free, and edge device-compatible hypervector encoding. In *DATE*, pp. 1–2, 2023.
- [130] J. Orchard and R. Jarvis. Hyperdimensional computing with spiking-phaser neurons, 2023.
- [131] Z. Zou *et al.* Memory-inspired spiking hyperdimensional network for robust online learning. *Scientific Reports*, 12(1):7641, May 2022.
- [132] G. Bent *et al.* Hyperdimensional computing using time-to-spike neuromorphic circuits. In *IJCNN*, pp. 1–8, 2022.
- [133] O. Räsänen. Generating hyperdimensional distributed representations from continuous-valued multivariate sensory input. 07 2015.
- [134] G. Karunaratne *et al.* Real-time language recognition using hyperdimensional computing on phase-change memory array. In *IEEE AICAS*, 2021.
- [135] Y. Kim *et al.* Geniehd: Efficient dna pattern matching accelerator using hyperdimensional computing. In *DATE*, pp. 115–120, 2020.
- [136] F. Cumbo *et al.* A brain-inspired hyperdimensional computing approach for classifying massive dna methylation data of cancer. *Algorithms*, 13(9), 2020.
- [137] Z. Zou *et al.* Biohd: An efficient genome sequence search platform using hyperdimensional memorization. In *ISCA*, pp. 656–669, 2022.
- [138] S. Gupta *et al.* Rapid: A reram processing in-memory architecture for dna sequence alignment. In *ISLPED*, pp. 1–6, 2019.
- [139] P. Poduval *et al.* Cognitive correlative encoding for genome sequence matching in hyperdimensional system. In *DAC*, pp. 781–786, 2021.
- [140] S. Liu and J. Han. Toward energy-efficient stochastic circuits using parallel sobol sequences. *IEEE Trans. Very Large Scale Integr. Syst.*, 26(7), 2018.
- [141] S. Liu and J. Han. Energy efficient stochastic computing with sobol sequences. In *2017 DATE*, pp. 650–653, 2017.
- [142] M. H. Najafi *et al.* Performing stochastic computation deterministically. *IEEE TVLSI*, 27(12):2925–2938, 2019.
- [143] A. Hernández-Cano *et al.* Onlinehd: Robust, efficient, and single-pass online learning using hyperdimensional system. In *DATE*, pp. 56–61, 2021.
- [144] T. A. Plate. A common framework for distributed representation schemes for compositional structure. In *Connectionist Systems for Knowledge Representation and Deduction*, pp. 15–34, 1997.
- [145] K. Schlegel *et al.* A comparison of vector symbolic architectures. *Artificial Intelligence Review*, 55(6):4523–4555, Aug 2022.
- [146] A. Rahimi *et al.* High-dimensional computing as a nanoscalable paradigm. *IEEE TCAS I*, 64(9):2508–2521, 2017.
- [147] D. Kleyko *et al.* Vector symbolic architectures as a computing framework for emerging hardware. *Proceedings of the IEEE*, 110(10):1538–1571, 2022.
- [148] S. Datta *et al.* A programmable hyper-dimensional processor architecture for human-centric iot. *IEEE JESTCS*, 9(3):439–452, 2019.
- [149] L. Ge and K. K. Parhi. Classification using hyperdimensional computing: A review. *IEEE Circuits and Systems Magazine*, 20(2):30–47, 2020.
- [150] S. Salamat *et al.* F5-hd: Fast flexible fpga-based framework for refreshing hyperdimensional computing. In *Proceedings of the 2019 ACM/SIGDA International Symposium on Field-Programmable Gate Arrays*, FPGA '19, pp. 53–62, 2019.
- [151] D. Rachkovskij *et al.* Sparse binary distributed encoding of scalars. *Journal of Automation and Information Sciences*, 37:12–23, 01 2005.
- [152] M. Schmuck *et al.* Hardware optimizations of dense binary hyperdimensional computing: Rematerialization of hypervectors, binarized bundling, and combinational associative memory. *J. Emerg. Technol. Comput. Syst.*, 15(4), oct 2019.
- [153] D. A. Rachkovskij *et al.* Building a world model with structure-sensitive sparse binary distributed representations. *Biologically Inspired Cognitive Architectures*, 3:64–86, 2013.
- [154] M. Imani *et al.* Low-power sparse hyperdimensional encoder for language recognition. *IEEE Design & Test*, 34(6):94–101, 2017.
- [155] D. Haputhanthri *et al.* Evaluating complex sparse representation of hypervectors for unsupervised machine learning. In *IJCNN*, pp. 1–6, 2022.
- [156] T. I. Cannings and R. J. Samworth. Random-projection ensemble classification, 2015.
- [157] A. Thomas *et al.* A theoretical perspective on hyperdimensional computing. *J. Artif. Int. Res.*, 72:215–249, jan 2022.
- [158] M. Sahlgrén. An introduction to random indexing. In *TKE*, Copenhagen, Denmark, 2005.
- [159] A. Rahimi and B. Recht. Random features for large-scale kernel machines. In *ANIPS*, volume 20. Curran Associates, Inc., 2007.
- [160] B. Schölkopf. The kernel trick for distances. In *Proceedings of the 13th ICNIPS, NIPS'00*, pp. 283–289, Cambridge, MA, USA, 2000. MIT Press.
- [161] A. Hernández-Cano *et al.* A framework for efficient and binary clustering in high-dimensional space. In *DATE*, pp. 1859–1864, 2021.
- [162] J. Wang *et al.* Disthd: A learner-aware dynamic encoding method for hyperdimensional classification, 2023.
- [163] Z. Zou *et al.* Scalable edge-based hyperdimensional learning system with brain-like neural adaptation. In *SC21: International Conference for High Performance Computing, Networking, Storage and Analysis*, pp. 1–15, 2021.
- [164] Z. Zou *et al.* Manihd: Efficient hyper-dimensional learning using manifold trainable encoder. In *DATE*, pp. 850–855, 2021.
- [165] D. Kleyko *et al.* Holographic graph neuron: A bioinspired architecture for pattern processing. *IEEE TNNLS*, 28(6):1250–1262, 2017.
- [166] B. Khaleghi *et al.* Shearer: Highly-efficient hyperdimensional computing by software-hardware enabled multifold approximation. In *ISLPED, ISLPED '20*, pp. 241–246, 2020.
- [167] A. Hernández-Cano *et al.* Prid: Model inversion privacy attacks in hyperdimensional learning systems. In *2021 58th ACM/IEEE Design Automation Conference (DAC)*, pp. 553–558, 2021.
- [168] M. Imani *et al.* Semihd: Semi-supervised learning using hyperdimensional computing. In *ICCAD*, pp. 1–8, 2019.
- [169] R. Wang *et al.* Enhdc: Ensemble learning for brain-inspired hyperdimensional computing. *IEEE Embedded Systems Letters*, 15(1):37–40, 2023.
- [170] C.-Y. Chang *et al.* Task-projected hyperdimensional computing for multi-task learning. In *AIAI*, pp. 241–251, Cham, 2020.
- [171] J. Kang *et al.* Xcelhd: An efficient gpu-powered hyperdimensional computing with parallelized training. In *ASP-DAC*, pp. 220–225. IEEE, 2022.
- [172] J. Kang *et al.* Relhd: A graph-based learning on fetef with hyperdimensional computing. In *ICCD*, pp. 553–560, 2022.
- [173] M. Imani *et al.* Revisiting hyperdimensional learning for fpga and low-power architectures. In *2021 IEEE International Symposium on High-Performance Computer Architecture (HPCA)*, pp. 221–234, 2021.
- [174] K. Huch *et al.* Superconducting hyperdimensional associative memory circuit for scalable machine learning. *IEEE Trans. on Applied Superconductivity*, 33(5):1–14, 2023.
- [175] M. Imani *et al.* Exploring hyperdimensional associative memory. In *2017 IEEE International Symposium on High Performance Computer Architecture (HPCA)*, pp. 445–456, 2017.
- [176] T. F. Wu *et al.* Brain-inspired computing exploiting carbon nanotube fetes and resistive ram: Hyperdimensional computing case study. In *2018 IEEE International Solid - State Circuits Conference - (ISSCC)*, pp. 492–494, 2018.
- [177] Y. Kim *et al.* Cascadehd: Efficient many-class learning framework using hyperdimensional computing. In *2021 58th ACM/IEEE Design Automation Conference (DAC)*, pp. 775–780. IEEE Press, 2021.
- [178] A. Safa *et al.* Supporthd: Hyperdimensional computing with scalable hypervector sparsity. In *NICE*, pp. 20–25, 2023.
- [179] Y. Ni *et al.* Neurally-inspired hyperdimensional classification for efficient and robust biosignal processing. In *ICCAD, ICCAD'22*, 2022.
- [180] M. Imani *et al.* Sparsehd: Algorithm-hardware co-optimization for efficient high-dimensional computing. In *2019 IEEE 27th Annual International Symposium on Field-Programmable Custom Computing Machines (FCCM)*, pp. 190–198, 2019.
- [181] J. Morris *et al.* Comphd: Efficient hyperdimensional computing using model compression. In *ISLPED*, pp. 1–6, 2019.
- [182] S. Salamat *et al.* Accelerating hyperdimensional computing on fpgas by exploiting computational reuse. *IEEE TComp*, 69(8):1159–1171, 2020.
- [183] D. Kleyko *et al.* Hyperdimensional computing in industrial systems: The use-case of distributed fault isolation in a power plant. *IEEE Access*, 6:30766–30777, 2018.
- [184] M. Imani *et al.* A framework for collaborative learning in secure high-dimensional space. In *CLOUD*, pp. 435–446, 2019.
- [185] M. Imani *et al.* Fach: Fpga-based acceleration of hyperdimensional computing by reducing computational complexity. In *Proceedings of the 24th Asia and South Pacific Design Automation Conference, ASPDAC '19*, pp. 493–498, 2019.
- [186] F. Montagna *et al.* Pulp-hd: Accelerating brain-inspired high-dimensional computing on a parallel ultra-low power platform. In *2018 55th ACM/ESDA/IEEE Design Automation Conference (DAC)*, pp. 1–6, 2018.
- [187] J. Morris *et al.* Hyperspike: Hyperdimensional computing for more efficient and robust spiking neural networks. In *DATE*, pp. 664–669, 2022.
- [188] R. Chandrasekaran *et al.* Fhdnn: Communication efficient and robust federated learning for aiot networks. In *DAC, DAC '22*, pp. 37–42, 2022.
- [189] J. Morris *et al.* Multi-label hd classification in 3d flash. In *VLSI-SOC*, pp. 10–15, 2020.
- [190] A. Mitrokhin *et al.* Learning sensorimotor control with neuromorphic sensors: Toward hyperdimensional active perception. *Science Robotics*, 4(30):eaaw6736, 2019.
- [191] A. Menon *et al.* A highly energy-efficient hyperdimensional computing processor for wearable multi-modal classification. In *BioCAS*, pp. 1–4, 2021.
- [192] A. Rosato *et al.* Hyperdimensional computing for efficient distributed classification with randomized neural networks. In *IJCNN*, pp. 1–10, 2021.
- [193] O. Räsänen and S. Kakouros. Modeling dependencies in multiple parallel data streams with hyperdimensional computing. *IEEE Signal Processing Letters*, 21(7):899–903, 2014.
- [194] W. Xu *et al.* Fsl-hd: Accelerating few-shot learning on reram using hyperdimensional computing. In *DATE*, pp. 1–6, 2023.
- [195] J. B. Travník and P. M. Pilarski. Representing high-dimensional data to intelligent prostheses and other wearable assistive robots: A first comparison of tile coding and selective kanerva coding. In *ICORR*, pp. 1443–1450. IEEE, 2017.
- [196] Y. Kaya *et al.* 1d-local binary pattern based feature extraction for classification of epileptic eeg signals. *Applied Mathematics and Computation*, 243:209–219, 2014.
- [197] Y. Cao *et al.* Deep quantization network for efficient image retrieval. *AAAI*, 2016.
- [198] H. Zhu *et al.* Deep hashing network for efficient similarity retrieval. *AAAI*, 2016.
- [199] Y. Cao *et al.* Deep visual-semantic quantization for efficient image retrieval. In *CVPR*, 2017.
- [200] Y. Cao *et al.* Deep cauchy hashing for hamming space retrieval. In *CVPR*, 2018.
- [201] B. Liu *et al.* Deep triplet quantization. *MM, ACM*, 2018.
- [202] P. Koehn. Europarl. <http://www.statmt.org/europarl/>, 2005.
- [203] S. Joe and F. Y. Kuo. Remark on algorithm 659: Implementing sobol's quasirandom sequence generator. *ACM Trans. Math. Softw.*, 29(1), 2003.
- [204] S. Liu and J. Han. Toward energy-efficient stochastic circuits using parallel sobol sequences. *IEEE TVLSI*, 26(7):1326–1339, 2018.

- [205] A. Alaghi *et al.* The promise and challenge of stochastic computing. *IEEE Transactions on Computer-Aided Design of Integrated Circuits and Systems*, 37(8):1515–1531, 2018.
- [206] M. H. Najafi. *New views for stochastic computing: From time-encoding to deterministic processing.* PhD thesis, University of Minnesota, Minneapolis, USA, 2018.
- [207] M. Alawad and M. Lin. Survey of stochastic-based computation paradigms. *IEEE Transactions on Emerging Topics in Computing*, 7(1):98–114, 2019.
- [208] M. H. Najafi and M. E. Salehi. A Fast Fault-Tolerant Architecture for Sauvola Local Image Thresholding Algorithm Using Stochastic Computing. *IEEE Transactions on Very Large Scale Integration (VLSI) Systems*, 24(2):808–812, Feb 2016.
- [209] M. H. Najafi *et al.* Low-Cost Sorting Network Circuits Using Unary Processing. *IEEE Trans. on Very Large Scale Integration (VLSI) Systems*, 26(8):1471–1480, Aug 2018.
- [210] Y. Liu *et al.* A survey of stochastic computing neural networks for machine learning applications. *IEEE Transactions on Neural Networks and Learning Systems*, 32(7):2809–2824, 2021.
- [211] S. R. Faraji *et al.* Energy-efficient convolutional neural networks with deterministic bit-stream processing. In *2019 Design, Automation Test in Europe Conference Exhibition (DATE)*, pp. 1757–1762, 2019.
- [212] S. Zhang *et al.* Assessing robustness of hyperdimensional computing against errors in associative memory. In *ASAP*, pp. 211–217, 2021.
- [213] H. V. Weyl. Über die gleichverteilung von zahlen mod. eins. *Mathematische Annalen*, 77:313–352, 1916.
- [214] The Unreasonable Effectiveness of Quasirandom Sequences — Extreme Learning — extremelearning.com.au/unreasonable-effectiveness-of-quasirandom-sequences/. [Accessed 10-May-2023].
- [215] Weight Distribution Formula for Some Class of Cyclic Codes — IDEALS — [ideals.illinois.edu. https://www.ideals.illinois.edu/items/100041](https://www.ideals.illinois.edu/items/100041). [Accessed 10-May-2023].
- [216] M. D. McKay *et al.* Comparison of the three methods for selecting values of input variable in the analysis of output from a computer code. 21, 5 1979.
- [217] R. Gold. Optimal binary sequences for spread spectrum multiplexing. *IEEE Transactions on Inf. The.*, 13(4):619–621, 1967.
- [218] J. L. Walsh. A closed set of normal orthogonal functions. *American Journal of Mathematics*, 45(1):5–24, 1923.
- [219] H. Faure. Variations on $(0, s)$ -sequences. *Journal of Complexity*, 17(4):741–753, Dec 2001.
- [220] J. M. Hammersley and D. C. Handscomb. *Monte Carlo Methods*. Springer Netherlands, 1964.
- [221] H.-J. Zepernick and A. Finger. *Binary Pseudo Random Sequences*, chapter 4, pp. 87–125. John Wiley & Sons, Ltd, 2005.
- [222] L. Kuipers and H. Niederreiter. *Uniform Distribution of Sequences*. Dover Books on Mathematics. Dover Publications, Mineola, NY, May 2006.
- [223] H. Niederreiter and C. Xing. Low-discrepancy sequences and global function fields with many rational places. *Finite Fields and Their Applications*, 2(3):241–273, 1996.
- [224] R. L. Cook. Stochastic sampling in computer graphics. *ACM Trans. Graph.*, 5:51–72, 1988.
- [225] J. G. van der Corput. Verteilungsfunktionen. I. *Proc. Akad. Wet. Amsterdam*, 38:813–821, 1935.
- [226] L. Marohnic and T. Srirnevcki. Plastic number: Construction and applications. 2012.
- [227] C. D. Lin and B. Tang. Latin hypercubes and space-filling designs, 2022.
- [228] I. Krykova. Evaluating of path-dependent securities with low discrepancy methods. Master’s thesis, Worcester Polytechnic Institute, January 2004.
- [229] I. L. Dalal *et al.* Low discrepancy sequences for monte carlo simulations on reconfigurable platforms. In *ASAP*, pp. 108–113, Los Alamitos, CA, USA, 2008.
- [230] R. Lidl and H. Niederreiter. *Finite Fields*. Number v. 20, pt. 1 in EBL-Schweitzer. Cambridge University Press, 1997.
- [231] Y. Khan *et al.* A new frontier of printed electronics: Flexible hybrid electronics. *Advanced Materials*, 32(15):1905279, 2020.
- [232] T. Anthony. Streaming encoding algorithms for scalable hyperdimensional computing, 2023.
- [233] M. Heddes *et al.* Hyperdimensional hashing: A robust and efficient dynamic hash table. In *DAC*, pp. 907–912, 2022.
- [234] F. Neugebauer *et al.* Building a better random number generator for stochastic computing. In *2017 Euromicro Conference on Digital System Design (DSD)*, pp. 1–8, 2017.
- [235] A. Alaghi and J. P. Hayes. Exploiting correlation in stochastic circuit design. In *ICCD*, pp. 39–46, Asheville, NC, USA, 2013.
- [236] R. Chandrasekaran and M. Heddes. hyperdimensional-computing. <https://github.com/hyperdimensional-computing/torchhd>, 2022. date accessed: 01-21-2023.
- [237] Hdlib, 2019. <https://github.com/skurella/hdlib> [Accessed: 07/20/2023].
- [238] Pybhv, 2023. <https://github.com/Adam-Vandervorst/PyBHV> [Accessed: 07/26/2023].
- [239] Hd-classification, 2023. <https://github.com/UCSD-SEELab/HD-Classification> [Accessed: 07/26/2023].
- [240] M. Hersche *et al.* Constrained few-shot class-incremental learning. In *Proceedings of the IEEE Conference on Computer Vision and Pattern Recognition (CVPR)*, 2022.
- [241] A. from several public and private organizations. Semantic vectors package. <https://github.com/semanticvectors/semanticvectors/wiki>, 2017, date accessed: 01-22-2023.
- [242] M. Hersche *et al.* constrained-fscil. <https://github.com/IBM/constrained-FSCIL>, 2022. date accessed: 01-22-2023.



Sercan Aygun (S’09-M’22) received a B.Sc. degree in Electrical & Electronics Engineering and a double major in Computer Engineering from Eskisehir Osmangazi University, Turkey, in 2013. He completed his M.Sc. degree in Electronics Engineering from Istanbul Technical University in 2015 and a second M.Sc. degree in Computer Engineering from Anadolu University in 2016. Dr. Aygun received his Ph.D. in Electronics Engineering from Istanbul Technical University in 2022. Dr. Aygun’s Ph.D. work has appeared in several Ph.D. Forums of top-tier conferences, such as DAC, DATE, and ESWEK. He received the Best Scientific Research Award of the ACM SIGBED Student Research Competition (SRC) ESWEK 2022 and the Best Paper Award at GLSVLSI’23. Dr. Aygun has been selected for the MLCommons Rising Stars program in Machine Learning and Systems Research in 2023. He is currently a postdoctoral researcher at the University of Louisiana at Lafayette, USA. He works on emerging computing technologies, including stochastic computing in computer vision and machine learning.



Mehran Shoushtari Moghadam (S’22) received the B.Sc. degree in Computer Engineering - Hardware and the M.Sc. degree in Computer Engineering - Computer Architecture from the University of Isfahan, Iran, in 2010 and 2016 respectively. He is currently pursuing the Ph.D degree with the Center for Advanced Computer Studies, School of Computing and Informatics, University of Louisiana at Lafayette, LA, USA. His research interests include Wireless Networks, Signal Processing, Computer Architecture, VLSI design, Approximate Computing, Stochastic Computing and Brain-Inspired Computing.



M. Hassan Najafi (S’15-M’18) received the B.Sc. degree in Computer Engineering from the University of Isfahan, Iran, the M.Sc. degree in Computer Architecture from the University of Tehran, Iran, and the Ph.D. degree in Electrical Engineering from the University of Minnesota, Twin Cities, USA, in 2011, 2014, and 2018, respectively. He is currently an Assistant Professor at the School of Computing and Informatics, University of Louisiana, LA, USA. His research interests include stochastic and approximate computing, unary processing, in-memory computing, and hyperdimensional computing. He has authored/co-authored more than 60 peer-reviewed papers and has been granted 5 U.S. patents with more pending. In recognition of his research, he received the 2018 EDAA Outstanding Dissertation Award, the Doctoral Dissertation Fellowship from the University of Minnesota, and the Best Paper Award at the ICCD’17 and GLSVLSI’23. Dr. Najafi has been an editor for the IEEE Journal on Emerging and Selected Topics in Circuits and Systems.



Mohsen Imani (Member, IEEE) received the Ph.D. degree from the Department of Computer Science, UC San Diego. He is currently an Assistant Professor at the Department of Computer Science, UC Irvine. He is also the Director of the Bio-Inspired Architecture and Systems (BIASLab). His contribution has led to a new direction in brain-inspired hyperdimensional computing that enables ultra-efficient and real-time learning and cognitive support. His research was also the main initiative in opening up multiple industrial and governmental research programs. His research has been recognized with several awards, including the Bernard and Sophia Gordon Engineering Leadership Award, the Outstanding Researcher Award, and the Powell Fellowship Award. He also received the Best Doctorate Research from UCSD and several best paper nomination awards at multiple top conferences, including Design Automation Conference (DAC) in 2019 and 2020, Design Automation and Test in Europe (DATE) in 2020, and International Conference on Computer-Aided Design (ICCAD) in 2020. Furthermore, he received the Best Paper Award at the DATE 2022 Conference.